DNA Damage Activates a Spatially Distinct Late Cytoplasmic Cell-Cycle Checkpoint Network Controlled by MK2-Mediated RNA Stabilization

H. Christian Reinhardt,[1,6,7,8] Pia Hasskamp,[1,10,11] Ingolf Schmedding,[1,10,11] Sandra Morandell,[1] Marcel A.T.M. van Vugt,[5] XiaoZhe Wang,[9] Rune Linding,[4] Shao-En Ong,[2] David Weaver,[9] Steven A. Carr,[2] and Michael B. Yaffe[1,2,3,*]

[1]David H. Koch Institute for Integrative Cancer Research, Department of Biology, Massachusetts Institute of Technology, Cambridge, MA 02132, USA
[2]Broad Institute of MIT and Harvard, Cambridge, MA 02132, USA
[3]Center for Cell Decision Processes, Department of Biological Engineering, Massachusetts Institute of Technology, Cambridge, MA 02132, USA
[4]Institute of Cancer Research, London SW3 6JB, UK
[5]Department of Medical Oncology, University Medical Centre Groningen, Groningen 9700 RB, The Netherlands
[6]Department of Internal Medicine, Division I, University Hospital Cologne, Cologne 50937, Germany
[7]Oncogene Signaling Group, Max Planck Institute Cologne, Cologne 50931, Germany
[8]Collaborative Research Center 832, Molecular Basis and Modulation of Cellular Interaction in the Tumor Microenvironment, Cologne 50937, Germany
[9]On-Q-ity, Waltham, MA 02451, USA
[10]These authors contributed equally to this work
[11]Present address: Medizinische Klinik 4, Universitätsklinik Köln, Germany
*Correspondence: myaffe@mit.edu
DOI 10.1016/j.molcel.2010.09.018

SUMMARY

Following genotoxic stress, cells activate a complex kinase-based signaling network to arrest the cell cycle and initiate DNA repair. p53-defective tumor cells rewire their checkpoint response and become dependent on the p38/MK2 pathway for survival after DNA damage, despite a functional ATR-Chk1 pathway. We used functional genetics to dissect the contributions of Chk1 and MK2 to checkpoint control. We show that nuclear Chk1 activity is essential to establish a G_2/M checkpoint, while cytoplasmic MK2 activity is critical for prolonged checkpoint maintenance through a process of posttranscriptional mRNA stabilization. Following DNA damage, the p38/MK2 complex relocalizes from nucleus to cytoplasm where MK2 phosphorylates hnRNPA0, to stabilize Gadd45α mRNA, while p38 phosphorylates and releases the translational inhibitor TIAR. In addition, MK2 phosphorylates PARN, blocking Gadd45α mRNA degradation. Gadd45α functions within a positive feedback loop, sustaining the MK2-dependent cytoplasmic sequestration of Cdc25B/C to block mitotic entry in the presence of unrepaired DNA damage. Our findings demonstrate a critical role for the MK2 pathway in the posttranscriptional regulation of gene expression as part of the DNA damage response in cancer cells.

INTRODUCTION

In response to DNA damage, eukaryotic cells activate a complex protein kinase-based checkpoint signaling network to arrest progression through the cell cycle. Activation of this signaling cascade recruits repair machinery to the sites of DNA damage, provides time for repair, or, if the damage is extensive, triggers programmed cell death or senescence (Abraham, 2001; Bartek and Lukas, 2003; Harper and Elledge, 2007; Jackson and Bartek, 2009; Reinhardt and Yaffe, 2009).

The canonical DNA damage response network can be divided into two major protein kinase signaling branches which function through the upstream kinases, ATM and ATR, respectively. These upstream kinases are critical initiators of the G_1/S, intra-S and G_2/M cell-cycle checkpoints through activation of their downstream effector kinases Chk2 and Chk1, respectively (Bartek and Lukas, 2003; Harper and Elledge, 2007; Jackson and Bartek, 2009; Kastan and Bartek, 2004; Shiloh, 2003). We and others have recently identified a third checkpoint effector pathway mediated by p38 and MAPKAP kinase-2 (MK2) that operates parallel to Chk1 and is activated downstream of ATM and ATR (Bulavin et al., 2001; Manke et al., 2005; Reinhardt et al., 2007). The p38/MK2 pathway is a global stress-response pathway (Kyriakis and Avruch, 2001) which, in response to genotoxic stress, becomes co-opted as part of the ATM/ATR-dependent cell-cycle checkpoint machinery (Raman et al., 2007; Reinhardt et al., 2007; Reinhardt and Yaffe, 2009). In particular, it is specifically within cells defective in the ARF-p53 pathway that cannot induce high levels of the Cdk inhibitor p21 that this p38/MK2 pathway becomes essential for proper cell-cycle control following DNA damage.

Chk1, Chk2, and MK2 appear to control the checkpoint response, at least in part, through the phosphorylation-dependent inactivation of members of the Cdc25 family of phosphatases, which are positive regulators of Cyclin/Cdk complexes (Donzelli and Draetta, 2003). Chk1, Chk2, and/or MK2-dependent phosphorylation of Cdc25B and C on Ser-323 and -216,

respectively, for example, creates binding sites for 14-3-3 proteins, resulting in modest catalytic inhibition and pronounced cytoplasmic sequestration of these mitotic phosphatases, preventing access to, and activation of, nuclear and centrosomal Cyclin/Cdk substrates (Boutros et al., 2007). Paradoxically, Chk1, Chk2, and MK2 phosphorylate the identical basophilic amino acid consensus motif on peptides, and all three kinases appear to exhibit similar activity against Cdc25B and C (Manke et al., 2005; O'Neill et al., 2002). Why then, at the systems level of cell-cycle control, do cells maintain more than one kinase to perform the same molecular function?

We reasoned that this diversity in kinase activity might involve specific differences in subcellular localization and/or timing in response to genotoxic stress. We therefore examined the spatial and temporal dynamics of DNA damage checkpoint signaling through the effector kinases Chk1 and MK2, and searched for additional MK2-specific targets relevant to checkpoint regulation. These studies surprisingly revealed that p53-defective cells contain two spatially and temporally distinct G_2/M checkpoint networks—an early "nuclear" checkpoint mediated through the actions of Chk1, and a late "cytoplasmic" checkpoint mediated through MK2. The critical cytoplasmic function of MK2 in late cell-cycle checkpoint control is the post-transcriptional modulation of gene expression through DNA damage-induced p38/MK2-dependent phosphorylation of RNA-binding/regulatory proteins. We show that p38/MK2-dependent phosphorylation of three key targets involved in RNA regulation, hnRNPA0, TIAR, and PARN, stabilizes an otherwise unstable Gadd45α transcript through its 3′UTR. The resulting accumulation of Gadd45α then functions, at the systems level, as part of a p38-dependent positive feedback loop to block the premature activation and nuclear translocation of Cdc25B and -C in the presence of ongoing DNA damage.

RESULTS

Chk1 and MK2 Control Early and Late G_2/M Checkpoints, Respectively, after DNA Damage

We recently demonstrated that depletion of the checkpoint kinase MK2 sensitizes p53-deficient cells to the effects of DNA-damaging chemotherapy (Reinhardt et al., 2007). A series of recent studies reported a similar requirement for Chk1 in p53-deficient cancer cells for survival after genotoxic stress (Chen et al., 2006; Koniaras et al., 2001; Mukhopadhyay et al., 2005). Paradoxically, Chk1 and MK2 phosphorylate the identical optimal sequence motif on their substrates (Manke et al., 2005), yet the enzymatic activity of both kinases is essential for proper cell-cycle control in response to DNA damage. To explore the mechanistic basis for these seemingly motif-identical kinases in DNA damage signaling, we used lentiviral shRNA to knock down Chk1 or MK2 in U2OS cells (see Figures S1A and S1B available online) and examined the kinetics of spontaneous checkpoint release after exposure to 1 μM doxorubicin for 1 hr. Cells were analyzed at 12, 18, 24, and 30 hr after doxorubicin treatment for mitotic accumulation by measuring DNA content and phosphohistone H3 (pHH3) positivity by flow cytometry in the presence of a nocodazole trap.

As shown in the upper panels of Figure 1A, knockdown of MK2 or Chk1 did not result in gross cell-cycle changes in the absence of DNA damage. Treatment of control cells with doxorubicin resulted in a gradual build-up of G_2-arrested cells over 24 hr, as evidenced by the accumulation of 4N cells staining negatively for pHH3 (Figure 1A, lower panels, and Figure 1B). Chk1-depleted cells, like wild-type cells, displayed a prominent 4N peak after DNA damage; however, by as early as 12 hr after doxorubicin, 7.7% of the cells already stained positively for pHH3. This percentage of pHH3-positive cells progressively rose to 15% by 18 hr and reached 25.6% and 29.5% by 24 and 30 hr, respectively, compared to 0.9% and 1.5% of the shRNA controls at these times. These latter pHH3 values for the Chk1 knockdown cells are similar to those seen in undamaged wild-type cells arrested in mitosis with nocodazole, and indicate an early failure of the G_2 checkpoint in Chk1-depleted cells.

In contrast to Chk1 depletion, examination of the MK2 knockdown cells showed an accumulation of 4N DNA-containing cells that were largely negative for pHH3 staining at 12 and 18 hr after doxorubicin (3.7% ± 1.2%, and 3.6% ± 0.5%, respectively), indicating a functional early G_2 arrest. However, by 24 and 30 hr following doxorubicin, a gradual collapse of the checkpoint was evident with 13.2% and 28.5% of MK2-depleted cells now staining positively for pHH3 (Figure 1B). Thus, MK2 depletion appeared to disrupt maintenance of the G_2 checkpoint at late times, whereas Chk1 depletion resulted in impaired checkpoint initiation and/or maintenance at earlier times. Expression of shRNA-resistant wild-type MK2 completely rescued the effect of MK2 depletion on doxorubicin-induced G_2/M arrest (Figures S2A–S2C), whereas expression of a kinase-dead MK2 mutant failed to restore these checkpoints, although this mutant bound to p38 (Figure S2D), confirming that MK2 activity itself was required for the late cell-cycle checkpoint arrest.

Distinct Nuclear and Cytoplasmic Locations of Active Chk1 and MK2 following DNA Damage Mediate Early and Late Checkpoint Functions

To investigate whether the different temporal kinetics of checkpoint escape seen in the Chk1- and MK2-deficient cells resulted from targeting spatially distinct substrate pools, we examined the subcellular localization of these two checkpoint kinases after genotoxic stress. Retroviral gene delivery was used to obtain stable low-level expression of GFP chimeras of Chk1 and MK2 in U2OS cells, and localization monitored in live cells before and after DNA damage over time. Both GFP-Chk1 and GFP-MK2 localized exclusively in the nucleus of resting cells, while GFP alone was diffusely distributed throughout both the cytoplasm and the nucleus (Figure 2A). Following doxorubicin, GFP-MK2 rapidly translocated from the nucleus to the cytoplasm, where it remained for at least 24 hr, whereas GFP-Chk1 remained nuclear. Phosphorylation/activation of the GFP fusion proteins following DNA damage occurred with identical kinetics as those seen for the endogenous Chk1 and MK2 (Figures 2B and 2C), with the damage-induced relocalization of MK2 completely dependent upon its activation by p38, since cytoplasmic translocation after doxorubicin was completely abolished by the addition of the p38 inhibitor SB203580

A
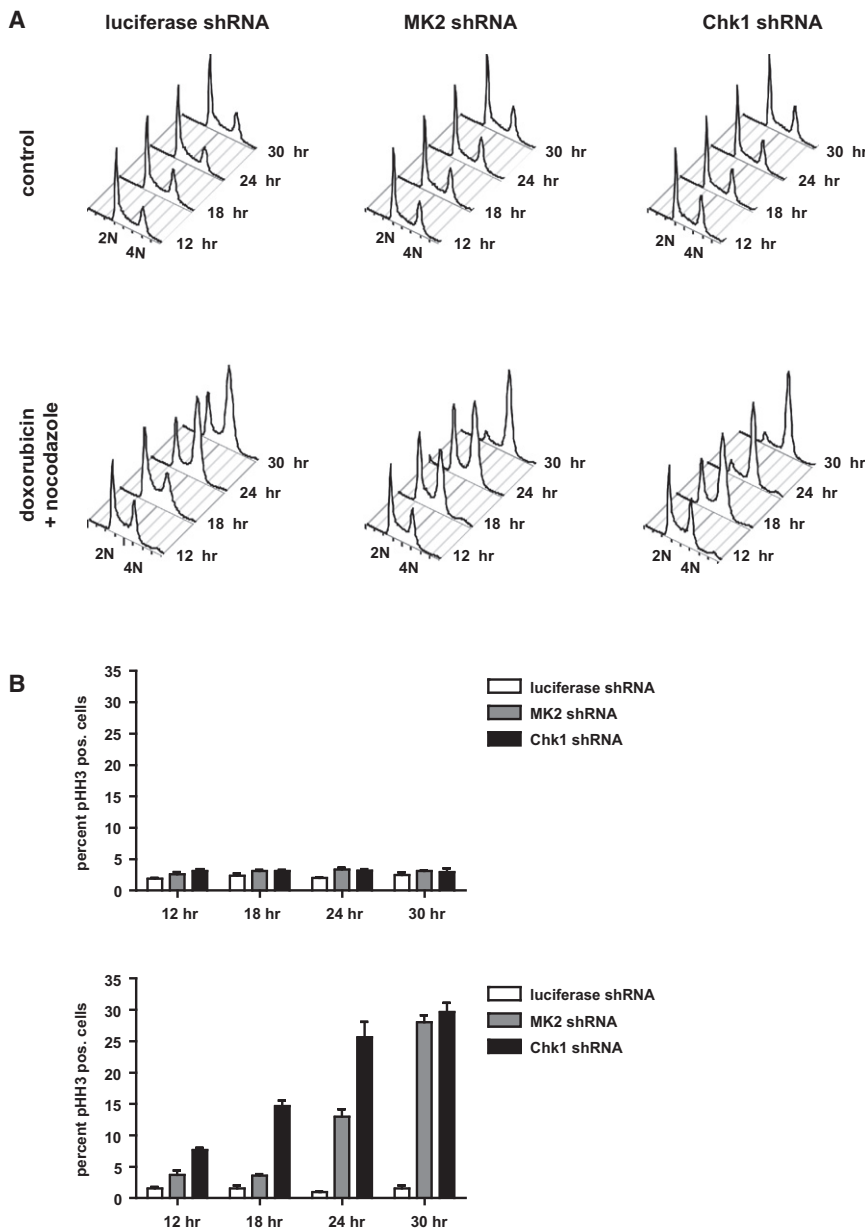
Figure 1. MK2 and Chk1 Control Temporally Distinct Components of the Cell-Cycle Checkpoint Response

(A) U2OS cells were infected with lentiviruses delivering luciferase-, MK2-, or Chk1-specific shRNAs (see also Figure S1). The ability of these cells to engage and maintain a functional cell-cycle checkpoint following genotoxic stress was analyzed using a FACS-based nocodazole trap experiment (Experimental Procedures). Knockdown of MK2 or Chk1 did not grossly affect the cell-cycle distribution of untreated cells (top panel). In response to 1 μM doxorubicin treatment for 1 hr, luciferase control shRNA-expressing cells mounted an intra-S and G2/M checkpoint response that remained stable for the 30 hr course of the experiment, as evidenced by the accumulation of a largely pHH3-negative 4N population (bottom panel, left, and B). MK2 shRNA-expressing cells initiated a functional intra-S, G2/M cell-cycle checkpoint that remained intact for at least 18 hr. At the 24 hr measurement, this checkpoint response started to decline with an increasing number of pHH3-positive cells showing a 4N DNA content, reflecting mitotically trapped cells (bottom panel, middle, and B). In contrast to the MK2 knockdown cells, which retained the ability to initiate a functional checkpoint response, cells that were depleted of Chk1 failed to initiate or maintain a checkpoint response within 12 hr following doxorubicin treatment (bottom panel, right, and B).

(B) Quantification of pHH3 staining of the samples shown in (A) (n = 7 experiments, mean values are shown with error bars indicating standard deviation).

B

mulation of MK2, while Chk1 remained exclusively nuclear. The DNA damage-induced cytoplasmic relocalization of MK2 could be completely prevented by caffeine (Figure 2F), indicating that the upstream kinases ATM and ATR mediate MK2 activation upon genotoxic stress. Pharmacological inhibition of the checkpoint effector kinase Chk1 using two different inhibitors, however, failed to prevent the doxorubicin-induced cytoplasmic localization of MK2, indicating that Chk1 and MK2 operate in separate parallel pathways (Figure 2F). Intriguingly, the activation and translocation of MK2, as well as phosphorylation of its cytoplasmic substrate, Hsp27, could also be observed in some human tumor samples which also displayed hallmarks of ongoing DNA damage (i.e., positive nuclear γH2AX staining), likely as a consequence of oncogenic stress (Figure 2G) (Bartkova et al., 2006; Di Micco et al., 2006).

To explore whether the distinct subcellular localizations of Chk1 and MK2 after DNA damage were directly responsible for early and late checkpoint arrest, we generated chimeric molecules in which each kinase was spatially substituted for the other within cells. MK2 contains both a bipartite nuclear localization

(Figure S3). Identical results were obtained following cisplatin treatment (Figure S3). To ensure that the visual behavior of GFP fusion proteins assayed in vivo reflected the subcellular localizations of endogenous Chk1 and MK2 kinases following DNA damage, a similar series of biochemical experiments was performed where the localization of endogenous activated Chk1 and MK2 was examined in cell lysates by nuclear and cytoplasmic fractionation. As shown in Figure 2D, endogenous phospho-MK2 became detectable in the cytoplasmic fraction shortly after DNA damage, while endogenous phospho-Chk1 remained in the nuclear fraction. In addition, we also used indirect immunofluorescence to directly monitor the subcellular localization of endogenous Chk1 and MK2 in situ (Figure 2E). These studies confirmed that doxorubicin induced robust cytoplasmic accu-

signal (NLS; amino acids 373–389) and a nuclear export signal (NES; amino acids 356–365) located near the C terminus (Figure 3Ai). In the kinase resting state, the NES is masked by a direct interaction with a hydrophobic patch in the kinase domain (ter Haar et al., 2007). Upon activation and MK2 phosphorylation on Thr-334 by p38, this interaction between the NES and the catalytic core is weakened and the NES becomes exposed, leading to cytoplasmic translocation (Ben-Levy et al., 1998; ter Haar et al., 2007). In contrast, Chk1 contains a NLS, but lacks a discernable NES (Figure 3Aii). Therefore, to produce an activatable but nuclear-restricted form of MK2, we expressed a construct in which the NES was functionally inactivated by insertion of point mutations (Figure 3Aiii). Similarly, to produce cytoplasmic forms of Chk1, we investigated constructs in which either the NLS was inactivated (Figure S4) or the NES motif from MK2 was inserted at the Chk1 N terminus (Figure 3Aiv). All constructs were fused to GFP to allow visualization of subcellular localization.

Constructs were expressed in asynchronously growing Chk1- or MK2-knockdown cells, which were left untreated or exposed to doxorubicin for 1 hr, followed by addition of nocodazole 2 hr after removal of doxorubicin, to capture cells escaping from DNA damage checkpoints in mitosis (Figure 3B). As an additional control, cells were treated with nocodazole alone. Cells were harvested 30 hr after doxorubicin and cell-cycle distribution assessed using FACS. As observed previously, treatment of cells expressing a control shRNA resulted in robust S and G_2/M checkpoints 30 hr after addition of doxorubicin, with G_2-arrested cells indicated by an accumulation of cells with 4N DNA content that were largely negative for pHH3 staining (Figure 3C). This arrest was completely abrogated in cells expressing a Chk1 shRNA (Figures 3B and 3C). However, MK2.ΔNES complementation of Chk1-depleted cells resulted in full restoration of functional S and G_2/M checkpoints, indicating that nuclear-targeted MK2 can functionally compensate for the loss of Chk1. Thus, a phospho-motif-related basophilic kinase activity within the nucleus is sufficient to re-establish functional checkpoint signaling in Chk1-defective cells.

In response to DNA damage, Chk1 is phosphorylated by ATR on Ser-317 and -345 in conserved SQ clusters, resulting in an increase of Chk1 kinase activity. We therefore asked whether forced expression of Chk1 in the cytoplasm could rescue checkpoint defects following loss of MK2. As we had observed earlier, knockdown of MK2 in U2OS cells abolished the doxorubicin-induced S and G_2/M cell-cycle checkpoints, evidenced by an accumulation of 21.3% mitotic cells with 4N DNA content staining positive for pHH3 that had escaped cell-cycle checkpoints during the 30 hr course of the experiment (Figures 3B and 3C). This value is similar to that of U2OS cells expressing a control shRNA that were blocked in mitosis with nocodazole, in the absence of DNA damage, indicating a complete loss of checkpoint function in MK2-depleted U2OS cells upon doxorubicin treatment. A cytoplasmic Chk1 construct was initially created by inactivating the Chk1 NLS through mutation of Arg-260/261/270/271 to Ala, resulting in a predominantly cytoplasmic accumulation of Chk1 (Chk1.ΔNLS) (Figure S4). We were surprised to observe that expression of this construct failed to rescue the checkpoint defects seen in MK2 knockdown cells. Addition

of leptomycin B, an inhibitor of Crm1-dependent nuclear export 12 hr prior to doxorubicin, however, did not result in nuclear entrapment of the Chk1.ΔNLS protein, indicating that this mutant could not shuttle between the cytoplasm and the nucleus, and was therefore unlikely to be activated by ATR following DNA damage (Figure S4). In contrast, leptomycin B treatment resulted in complete entrapment of MK2 within the nucleus despite doxorubicin-induced DNA damage (Figure S4B), demonstrating Crm1-dependent nuclear export of MK2 in response to DNA damage. We therefore created a second construct in which the MK2 NES was placed between GFP and the Chk1 cDNA. This NES.Chk1 construct, like Chk1.ΔNLS, also showed a predominantly cytoplasmic accumulation of Chk1 (Figure 3A). Importantly, however, this fusion protein was retained in the nucleus upon leptomycin B treatment, indicating that the NES.Chk1 fusion protein shuttles between cytoplasm and nucleus, where it can be directly activated upon DNA damage (Figure S4). Expression of this ATR-activatable, nucleocytoplasmic shuttling form of Chk1 completely rescued the checkpoint defects seen in U2OS cells lacking MK2 (Figures 3B and 3C). Notably, when this same Chk1.NES construct was mutated at Ser-317 and Ser-345 to prevent DNA damage-induced phosphorylation, it was unable to reverse the MK2 depletion phenotype, despite its cytoplasmic localization and nuclear-cytoplasmic shuttling. These data indicate that an activated cytoplasmic form of Chk1 can functionally compensate for the loss of MK2 activity.

Taken together, our findings indicate that Chk1 and MK2 control early and late DNA damage checkpoints, respectively, likely through phosphorylating distinct, spatially separated substrate pools following their activation by genotoxic stress. In agreement with this, our data indicate that either kinase can compensate for loss of the other, if the kinase activity is targeted to the proper subcellular locale.

MK2 and p38MAPK Activity Results in Long-Term Stabilization of Gadd45α through Phosphorylation of Proteins Involved in RNA Binding and Degradation

To identify likely substrates of MK2 that were critical for its late cytoplasmic checkpoint-maintaining function, we explored known roles for MK2 in other signaling contexts. In hematopoetic cells, MK2 is known to be involved in stabilizing unstable cytokine mRNAs (Gaestel, 2006), and we recently demonstrated a similar MK2-dependent stabilization of IL-1α in carcinoma cells following TNFα stimulation (Janes et al., 2008). Specifically, mRNAs containing AU-rich elements (AREs) in the 3′UTR have been shown to be stabilized in an MK2-dependent manner (Gaestel, 2006; Neininger et al., 2002). We therefore surveyed molecules potentially involved in cell-cycle control for the presence of 3′ AREs. Gadd45α, a cell-cycle regulator known to be induced after DNA damage in both a p53-dependent and -independent manner (Harkin et al., 1999; Kastan et al., 1992; Maekawa et al., 2008), emerged as a likely candidate among the molecules we identified. As shown in Figure 4A, Gadd45α mRNA was rapidly upregulated following doxorubicin-induced DNA damage, and accumulation of this mRNA was almost completely abolished when cells were depleted of MK2. However, upregulation of Gadd45α mRNA following genotoxic
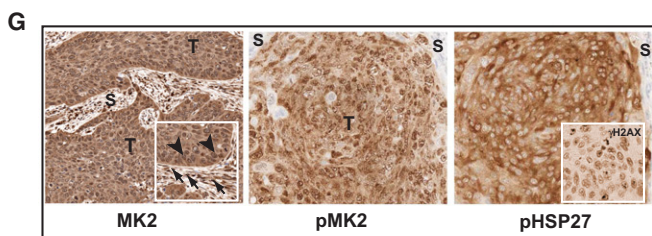
stress could be restored in MK2 knockdown cells if they were complemented with a cytoplasmic-localized form of Chk1.

To directly investigate the functional importance of DNA damage-induced Gadd45α induction, we used an RNAi approach (Figure 4B). Knockdown of Gadd45α in MK2-containing cells was found to result in premature collapse of both the doxorubicin-induced intra-S and G$_2$/M checkpoints by 30 hr after treatment (Figure 4B and Figure S1C), phenocopying the loss of checkpoint function in MK2 knockdown cells. These observations point to the importance of Gadd45α as a critical MK2 target for checkpoint regulation.

The 3′UTR of Gadd45α is heavily AU rich and contains numerous AREs, making posttranscriptional regulation through this part of the mRNA likely (Barreau et al., 2005). Importantly, under resting conditions, Gadd45α was recently shown to be actively degraded via a mechanism involving the 3′UTR (Lal et al., 2006). To conversely investigate whether a p38/MK2-dependent pathway(s) actively stabilizes Gadd45α mRNA levels through its 3′UTR, we used reporter constructs in which the GFP coding sequence was fused to the Gadd45α 3′UTR (GFP-3′UTR) (Lal et al., 2006) (Figures 4C and 4D). The GFP-3′UTR fusion construct, or GFP alone, was expressed in HeLa cells expressing either control or MK2-specific shRNA hairpins. As shown in Figures 4C and 4D, the basal levels of GFP protein were markedly lower in cells expressing the Gadd45α 3′UTR-chimeric mRNA than in cells expressing the unfused GFP mRNA. Cells expressing the 3′UTR chimeric GFP showed substantial induction of GFP following doxorubicin and UV treatment (∼9-fold), and milder upregulation after cisplatin exposure (∼4-fold), similar to what has been recently reported following MMS treatment (Lal et al., 2006). In marked contrast, the expression levels of the unfused GFP control protein remained unchanged. These results are consistent with regulation of Gadd45α mRNA levels through a posttranscriptional mechanism involving the 3′UTR.

Given the presence of AREs in the 3′UTR of Gadd45α, we speculated that MK2 might impose control over the Gadd45α mRNA via phosphorylation of RNA-binding proteins (RBPs) that recognize these sequences. To identify RBPs that might be involved in the posttranscriptional regulation of Gadd45α, we used Scansite (Obenauer et al., 2003) to examine known ARE-binding proteins for the presence of the MK2 consensus phosphorylation motif that we had defined previously using oriented peptide library screening (Manke et al., 2005). This revealed HuR, TTP, TIAR, and hnRNPA0 as likely MK2 candidate substrates. To investigate which of these proteins were bound to Gadd45α mRNA, we used RNA-IP followed by RT-PCR (Figures 5A and 5B). The IP conditions were optimized to retain the integrity of endogenous ribonucleoprotein (RNP) complexes. Subsequent RT-PCR analysis using Gadd45α-specific primers revealed prominent bands only from the TIAR and hnRNPA0 immunoprecipitate. No detectable amplification was seen in the control IgG IP or after IP with antibodies recognizing HuR or TTP. Importantly, we observed a reduction of Gadd45α mRNA binding to TIAR following doxorubicin exposure (Figure 5B). This observation is consistent with a known role for TIAR in translational inhibition (Anderson and Kedersha, 2002). On the other hand, Gadd45α mRNA levels in complex with hnRNPA0 appeared to be substantially increased after doxorubicin treatment (Figure 5B). Low-level but equal PCR products for GAPDH mRNA were seen in all of the IP samples tested; these signals likely represent the background binding of cellular mRNA to the IP reagents and hence served as a loading control.

To directly explore whether hnRNPA0 binds specifically to the 3′UTR of Gadd45α mRNA, we transfected the GFP-3′UTR hybrid

Figure 2. MK2 and Chk1 Localize to Distinct Subcellular Compartments following DNA Damage-Mediated Activation

(A) GFP, GFP.MK2, and GFP.Chk1 fusion constructs were expressed in U2OS cells. Following treatment with 10 μM doxorubicin, the same set of cells were imaged using real-time imaging. GFP.MK2 relocalized to the cytoplasm within 1 hr following addition of doxorubicin and remained largely cytoplasmic for 24 hr following genotoxic stress (top panel). GFP.Chk1 remained largely nuclear through the 24 hr course of the experiment (middle panel). Unfused GFP localized diffusely throughout the cytoplasm and the nucleus. (See also Figure S3.)

(B) The GFP.MK2 fusion protein is activated with the same kinetics, as endogenous wild-type MK2. Stably transfected U2OS cells were either mock treated or exposed to 10 μM doxorubicin as indicated. Following treatment, cells were lysed, and proteins were separated on SDS PAGE and visualized by immunoblot. MK2 activity was monitored with phospho-specific antibodies detecting p38-mediated activation/phosphorylation of Thr-334, located between the kinase domain and the C-terminal regulatory domain.

(C) The GFP.Chk1 fusion protein is activated with the same kinetics as endogenous wild-type Chk1. Cells were treated as in (B), and ATR-dependent phosphorylation on Ser-345 in the C-terminal regulatory region was monitored using immunoblotting.

(D) In response to doxorubicin, endogenously expressed MK2 and Chk1 show a biochemical relocalization pattern that is identical to their exogenously expressed GFP-fused counterparts (shown in A). Nuclear and cytoplasmic fractions were isolated using hypotonic lysis, and MK2 and Chk1 protein levels were determined using immunoblotting. Staining for tubulin (a cytoplasmic marker) and histone H1 (a nuclear marker) was performed to assess the purity of the isolated fractions.

(E) Indirect immunofluorescence staining was performed to verify the subcellular localization of endogenous MK2 and Chk1 in response to doxorubicin. Hoechst stain was used as a counterstain to provide a nuclear reference point. MK2 was predominantly localized in the cytoplasmic compartment 6 hr following doxorubicin exposure (top panel), while Chk1 remained nuclear (bottom panel).

(F) The doxorubicin-induced cytoplasmic relocalization of MK2 depends on a caffeine-sensitive kinase(s) but is independent of Chk1. U2OS cells were either left untreated or incubated with 10 μM doxorubicin for 6 hr, and the subcellular localization of MK2 was assessed by immunofluorescence as in (E). Doxorubicin treatment induced a robust translocation from the nucleus to the cytoplasm (upper two panels). This relocalization was completely prevented when cells were pretreated with 10 mM caffeine 30 min prior to doxorubicin application (middle panel). Inhibition of Chk1 with AZD-7762 (200 nM) or PF-477736 (5 μM) 30 min prior to doxorubicin failed to prevent cytoplasmic accumulation of MK2 (lower two panels).

(G) MK2 is activated in human tumor samples. Sections from human squamous cell head and neck cancer (T) and the surrounding stroma (S) were stained with antibodies against total MK2 (left panel), the activated/phosphorylated form of MK2 (middle panel), and its downstream substrate phospho-hsp27 (right panel). Of note, these tumors show spontaneous DNA damage as indicated by positive γH2AX staining (right panel inset), which correlates with MK2 activation and cytoplasmic accumulation of MK2 (left panel inset, arrowheads). In contrast, the stroma shows predominantly nuclear staining of MK2 (left panel inset, arrows) and minimal phospho-MK2 and phospho-hsp27 staining.
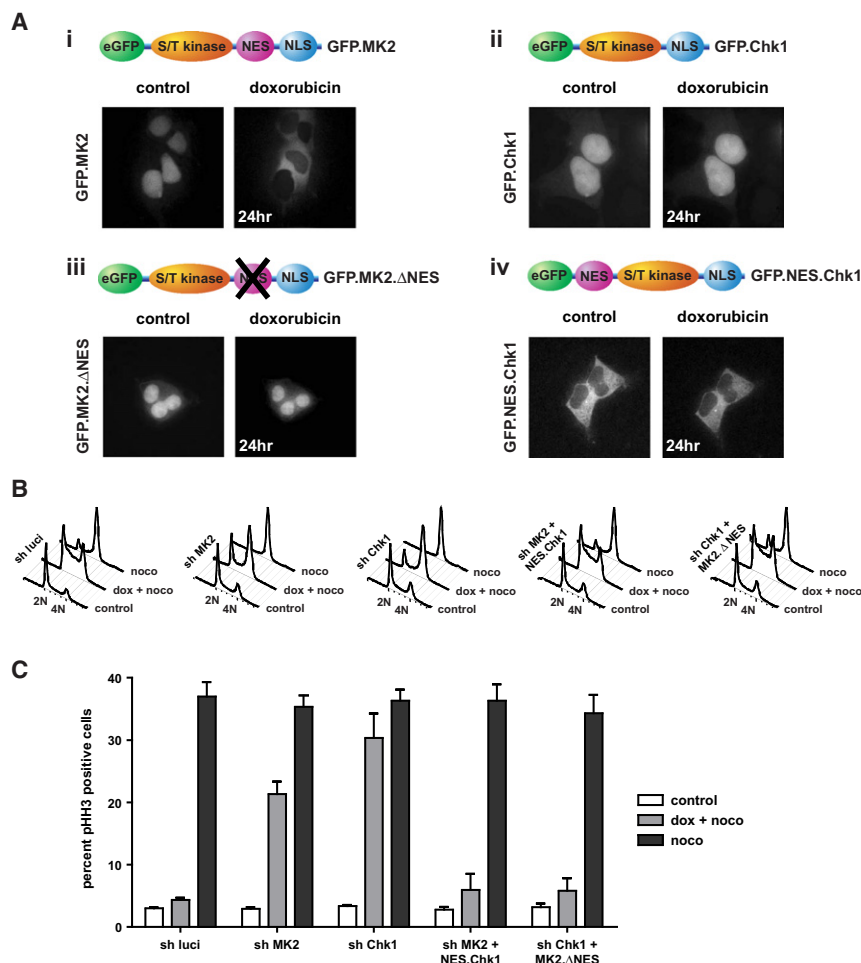
Figure 3. The Checkpoint Response following Doxorubicin Requires Early Nuclear and Late Cytoplasmic Basophilic Protein Kinase Activity

(A) MK2 and Chk1 localization mutants were generated as indicated. Live-cell images obtained before and 24 hr following treatment with 10 μM doxorubicin are shown below each construct. Of note, inactivation of the NES in MK2 results in a mutant with abolished ability to localize to the cytoplasm following genotoxic stress (Aiii). Fusion of the MK2 NES between GFP and Chk1 produces a Chk1 mutant that is localized primarily to the cytoplasm (Aiv).

(B and C) Shown is functional assessment of the ability of the localization mutants to establish and maintain cell-cycle checkpoints. U2OS cells were infected with lentiviruses expressing luciferase control shRNA, MK2-specific shRNA, or shRNA targeting Chk1. Knockdown cells were complemented with the localization mutants as indicated (see also Figure S2). Cells were treated with doxorubicin in a 30 hr nocodazole trap experiment, and cell-cycle profiles were assessed by FACS using DNA content profiles (B) and phosphohistone H3 staining (C). Of note, loss of nuclear Chk1 could be functionally compensated by expression of the GFP.MK2.ΔNES mutant that was relocalized to the nucleus, while loss of cytoplasmic MK2 could be rescued by expression of the GFP.NES.Chk1 mutant that was relocalized to the cytoplasm. (See also Figure S4.) Mean values are shown with error bars indicating standard deviation.

construct and repeated the hnRNPA0 IP. As we had observed for endogenous Gadd45α mRNA, treatment with doxorubicin induced a robust binding of eGFP mRNA fused to the Gadd45α-3′UTR (Figure 5C). These data strongly indicate that hnRNPA0 binds to endogenous Gadd45α mRNA via the 3′UTR in a DNA damage-inducible manner.

Next, to determine if hnRNPA0 was involved in the MK2-dependent checkpoint, we used a similar RNAi approach as that used to explore Gadd45α above. As shown in Figure 5D, knockdown of hnRNPA0 resulted in a substantial impairment of the intra-S- and G$_2$ checkpoint arrest following doxorubicin treatment, recapitulating, in part, what was observed in cells lacking MK2 or Gadd45α. hnRNPA0 has a single optimal phosphorylation site for MK2 on Ser-84 (Figure 5E) (Rousseau et al., 2002). However, it is unclear whether hnRNPA0 phosphorylation on Ser-84 is required for mRNA binding. We therefore transfected HeLa cells with HA-tagged hnRNPA0 or with a mutant form of hnRNPA0 in which Ser-84 was replaced with Ala (Figure 5F). Cells were either treated with doxorubicin or left untreated and lysed 12 hr later. hnRNPA0 was recovered by immunoprecipitation with an anti-HA-antibody, followed by RT-PCR analysis for bound Gadd45α mRNA using specific primers. This revealed a prominent Gadd45α mRNA band from hnRNPA0

wild-type-transfected MK2-proficient cells exposed to doxorubicin. In stark contrast, the interaction between hnRNPA0 and Gadd45α mRNA was almost entirely lost in cells transfected with the Ser-84 Ala mutant (Figure 5F, left panels). Similarly, no binding between hnRNPA0 and Gadd45α mRNA was seen in MK2-depleted cells (Figure 5F, middle panels). Importantly, expression of a cytoplasmic-targeted form of Chk1 restored DNA damage-stimulated hnRNPA0-Gadd45α mRNA binding and Gadd45α protein expression in MK2-depleted cells (Figure 5F, right panels), further supporting the notion that cytoplasmic checkpoint kinase activity is required for functional cell-cycle checkpoint control. These data strongly suggest a model in which long-term maintenance of DNA damage checkpoints involves MK2-dependent phosphorylation of hnRNPA0, stimulating its binding to the Gadd45α 3′UTR, with subsequent Gadd45α mRNA stabilization.

In contrast to hnRNPA0, we were unable to demonstrate MK2-dependent phosphorylation of TIAR. However, we did observe strong direct phosphorylation of TIAR by p38 in vitro (Figure 5G), together with a marked decrease in release of Gadd45α mRNA from TIAR following DNA damage in vivo if the cells were treated with the p38 inhibitor SB203580 (Figure 5H). These data argue that the combined actions of p38
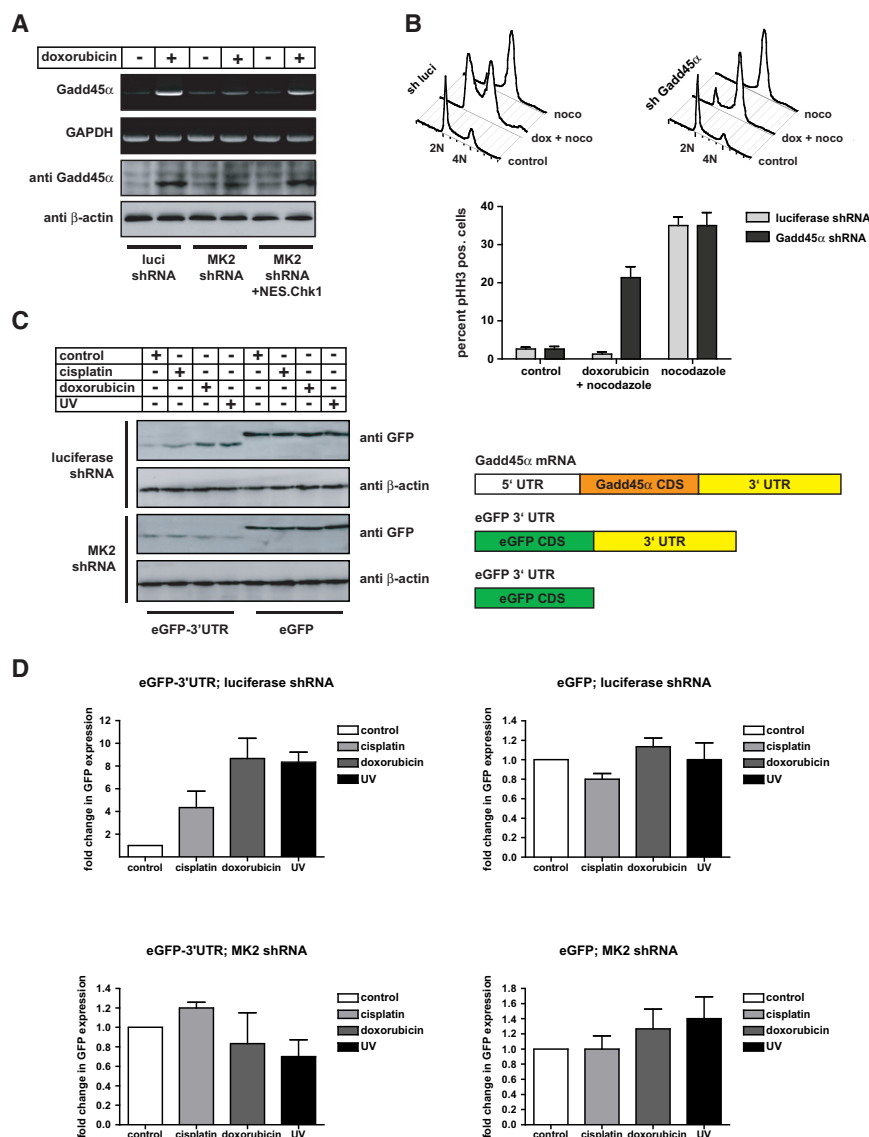
Figure 4. MK2 Is Essential to Stabilize Gadd45α mRNA and Protein Levels following Genotoxic Stress

(A) Loss of MK2 precludes doxorubicin-induced Gadd45α mRNA and protein upregulation. HeLa cells were infected with lentiviruses expressing luciferase control or MK2-specific shRNA. Cells were treated with 10 μM doxorubicin, and Gadd45α mRNA levels were examined by RT-PCR 18 hr later. Control cells robustly induced Gadd45α after doxorubicin exposure, while MK2-depleted cells failed to upregulate Gadd45α mRNA and protein in response to doxorubicin (left and middle panel). Of note, coexpression of the GFP.NES.Chk1 mutant that relocalized to the cytoplasm rescued the MK2 RNAi phenotype (right panel).

(B) Gadd45α depletion in functionally p53-deficient HeLa cells prevents the engagement of functional intra-S and G_2/M checkpoints following doxorubicin. HeLa cells expressing luciferase control shRNA or Gadd45α-specific hairpins were treated with doxorubicin (10 μM) in a 30 hr nocodazole trap experiment, and cell-cycle profiles were assessed by FACS. Control cells mounted a robust intra-S and G_2/M arrest in response to doxorubicin, as evidenced by an accumulation of 4N cells (monitored by PI staining) and a lack of pHH3 staining. In contrast, ~23% of Gadd45α-depleted cells entered mitosis throughout the 30 hr course of the experiment, indicating a bypass of the doxorubicin-induced cell-cycle arrest in these cells. Mean values are shown with error bars indicating standard deviation.

(C) Fusion of the Gadd45α mRNA 3′UTR to GFP confers MK2-dependent sensitivity to genotoxic stress for GFP protein expression. HeLa cells expressing luciferase control shRNA or MK2-specific hairpins were cotransfected with vectors encoding unfused eGFP or eGFP fused to the Gadd45α 3′UTR. In these experiments, the GFP-3′UTR protein is ~3 kD smaller than eGFP due to a deletion of 23 amino acids at the C terminus (Lal et al., 2006). Cells were mock treated or exposed to cisplatin (10 μM), doxorubicin (1 μM), or UV (20 J/m²), harvested 36 hr later, and GFP expression levels moni-tored by immunoblot. Expression levels of unfused GFP did not change following genotoxic stress; however, fusion of the Gadd45α 3′UTR to GFP resulted in repression of GFP expression that could be relieved upon genotoxic stress in a MK2-dependent manner. The right panel schematically depicts the endogenous Gadd45α transcript (top), the GFP-3′UTR fusion, and unfused GFP constructs.

(D) Relative GFP expression levels as shown in (C) were quantified from three independent experiments using ImageQuant software. Mean values are shown with error bars indicating standard deviation. Note the expanded y axis scale in panels 2–4.

and MK2 are responsible for the release of Gadd45α mRNA from TIAR and its accumulation and stabilization on hnRNPA0.

MK2-Mediated Phosphorylation of PARN Is Required to Prevent Gadd45α mRNA Degradation after Genotoxic Stress

The observation that MK2 is involved in regulation of Gadd45α expression through phosphorylation of mRNA-binding proteins prompted us to search for additional MK2 substrates that might be similarly involved in checkpoint signaling through posttranscriptional control of gene expression. To accomplish this, we used our previously published computational algorithms Scansite and NetworKIN (Linding et al., 2007; Obenauer et al., 2003)

to search mass spectrometry databases for phosphorylated proteins likely to be substrates of the p38/MK2 pathway. This analysis revealed poly-A ribonuclease PARN as a potential MK2 target. Phosphorylation of PARN on Ser-557 was previously identified in a large-scale mass spectrometry phosphoproteomic screen of human HeLa cells, but the functional relevance and responsible kinase are unknown. As shown in Figure 6A, recombinant wild-type PARN was strongly phosphorylated by MK2 in vitro; however, PARN in which Ser-557 was mutated to Ala showed dramatically reduced levels of phosphorylation, confirming that PARN can serve as a direct substrate for MK2, and demonstrating that Ser-557 is the dominant MK2 phosphorylation site.
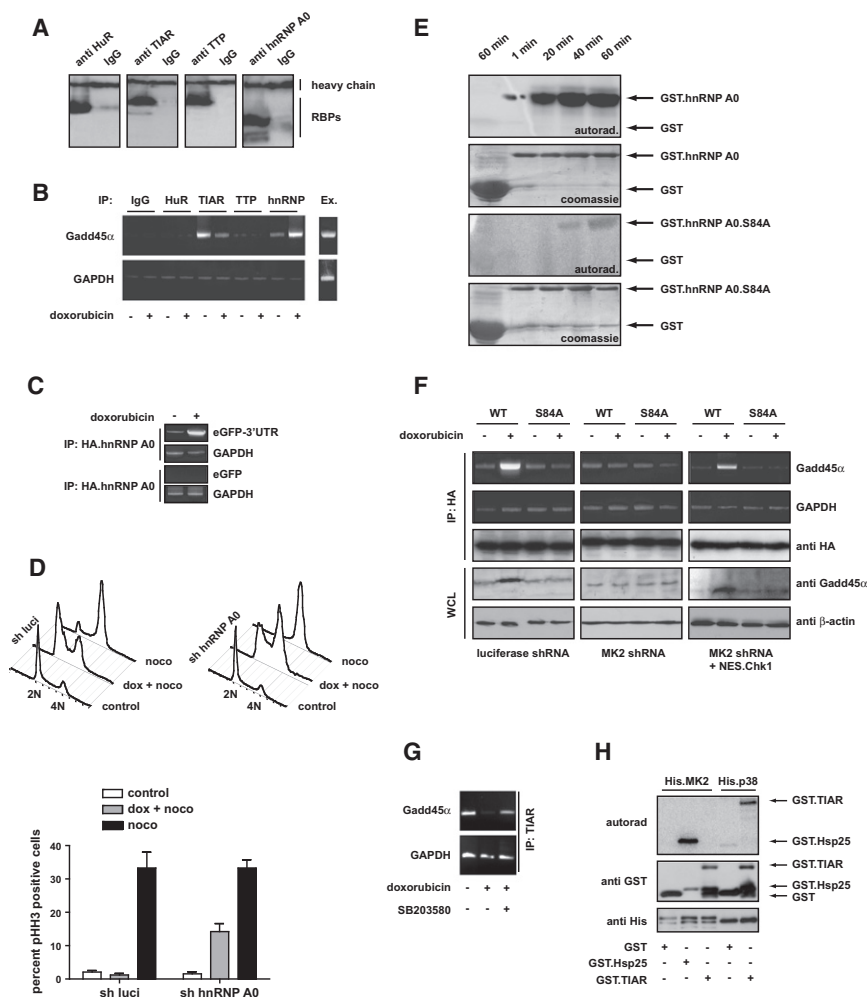
Figure 5. Doxorubicin Triggers MK2-Dependent Complex Formation between hnRNPA0 and the GADD45α mRNA 3′UTR, Resulting in GADD45α mRNA Stabilization and Increased GADD45α Protein Levels

(A) Immunoprecipitation followed by western blotting for the RBPs that were investigated.

(B) HeLa cells were either treated with doxorubicin (1 μM) for 12 hr or left untreated, lysed, and the binding of endogenous ARE-binding RBPs (HuR, TIAR, TTP, and hnRNPA0) to Gadd45α mRNA assessed using RNA-IP as described in the Experimental Procedures.

(C) hnRNPA0 interacts with the Gadd45a 3′UTR following genotoxic stress. HeLa cells were co-transfected with HA-tagged hnRNPA0 and either GFP fused to the Gadd45a 3′UTR or unfused GFP. Cells were treated with doxorubicin (10 μM) or vehicle for 12 hr, lysed, and HA.hnRNPA0 was immunoprecipitated followed by GFP RT-PCR. hnRNPA0 strongly boung to Gadd45α 3′UTR-fused GFP mRNA following doxorubicin. However, no interaction between hnRNPA0 and unfused GFP mRNA was detected, indicating that hnRNPA0 directly binds to the 3′UTR of Gadd45α mRNA.

(D) hnRNPA0 depletion in functionally p53-deficient HeLa cells prevents the engagement of a functional intra-S and G_2/M checkpoints following doxorubicin. HeLa cells expressing luciferase control shRNA or hnRNPA0-specific hairpins were treated with 10 μM doxorubicin in a 30 hr nocodazole trap experiment, and cell-cycle profiles were assessed by FACS. Control cells mounted a robust intra-S and G_2/M arrest in response to doxorubicin, as evidenced by an accumulation of 4N cells (monitored by PI staining), which were largely staining negative for pHH3. In contrast, ∼15% of hnRNPA0-depleted cells entered mitosis throughout the 30 hr course of the experiment, indicating a bypass of the doxorubicin-induced cell-cycle arrest in these cells. Mean values are shown with error bars indicating standard deviation.
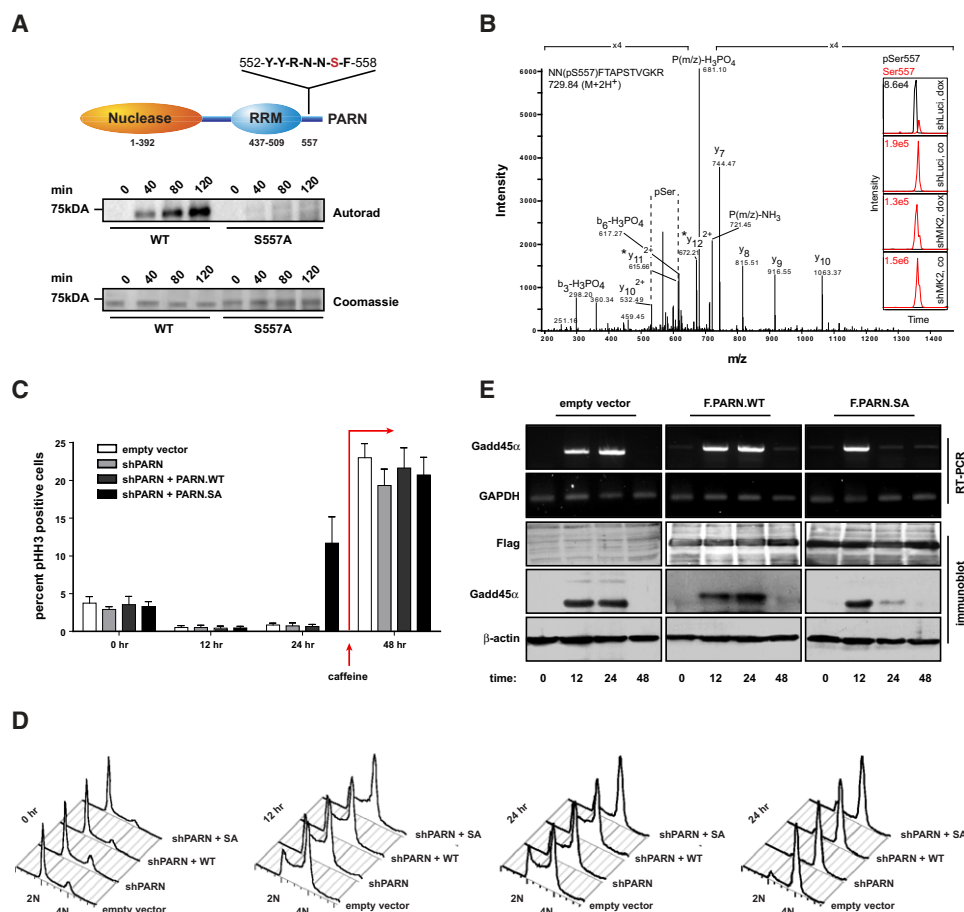
(E) Shown are in vitro kinase assays with bacterially purified recombinant MK2 and GST.hnRNPA0 wild-type or hnRNPA0 in which Ser-84 was mutated to Ala. GST served as a control. Following completion of the kinase assay, reaction mixtures were separated on SDS-PAGE and ^{32}P incorporation was visualized by autoradiography. GST.hnRNPA0 wild-type was readily phosphorylated by MK2 in vitro, while mutation of Ser-84 to Ala completely abolished hnRNPA0 phosphorylation.

(F) MK2-mediated hnRNPA0 phosphorylation on Ser-84 is essential for hnRNPA0 binding to Gadd45α mRNA. HeLa cells expressing luciferase control shRNA or MK2-specific shRNA were transfected with HA-tagged hnRNPA0 wild-type or the Ser-84 to Ala mutant. Cells were treated with doxorubicin (10 μM) or vehicle, lysed 12 hr later, and hnRNPA0 immunoprecipitated with anti HA-antibodies. While HA.hnRNPA0 readily coprecipitaed with Gadd45α mRNA following genotoxic stress in control cells, the Ser-84 to Ala mutant failed to interact with Gadd45α mRNA (left panel). This interaction was MK2-dependent, since hnRNPA0:Gadd45α mRNA complex formation was abolished in MK2-depleted cells (middle panel). Loss of MK2 could be rescued by expression of the activatable, cytoplasmic Chk1 mutant.

(G) Reduced binding of Gadd45α mRNA by TIAR following genotoxic stress depends on p38 activity. HeLa cells were treated with the p38 inhibitor SB203580 (10 μM) or vehicle 1 hr before treatment with doxorubicin as described in 5F. TIAR was immunoprecipitated followed by Gadd45α RT-PCR. TIAR binding to the Gadd45α mRNA that was abolished following genotoxic stress could be restored by inhibition of p38.

(H) In vitro kinase assays with bacterially purified recombinant His.MK2 or His.p38 and GST.TIAR. GST served as a control, and GST.Hsp25-peptide (AS 71–100) served as a positive control for MK2. Following completion of the kinase assay, reaction mixtures were separated on SDS-PAGE, and ^{32}P incorporation was visualized by autoradiography. GST.TIAR was readily phosphorylated by p38 in vitro after 20 min, but it was not phosphorylated by MK2.

To investigate whether MK2 phosphorylates PARN in vivo in response to genotoxic stress, we treated U2OS cells expressing either a luciferase or an MK2-specific shRNA with 10 μM doxorubicin. Four hours following doxorubicin, endogenous PARN was affinity purified from cell lysates and analyzed by mass spectrometry. As shown in Figure 6B, Ser-557-phosphorylated PARN peptides could not be detected in untreated U2OS cells expressing the luciferase control shRNA. In marked contrast, Ser-557-phosphorylated peptides were readily detected when these cells were treated with doxorubicin. This DNA damage-induced phosphorylation event was completely abolished in MK2-depleted cells, strongly suggesting that MK2 is the in vivo kinase directly responsible for genotoxic stress-induced PARN Ser-557 phosphorylation.

Figure 6. MK2 Directly Phosphorylates PARN on Ser-557 following Genotoxic Stress

(A) Shown are in vitro kinase assays using bacterially purified recombinant MK2 and 6xHis-tagged PARN wild-type or a PARN mutant in which Ser-557 was mutated to Ala. Following completion of the kinase assay, reaction mixtures were separated on SDS-PAGE and ^{32}P incorporation was visualized by autoradiography. Equal loading was confirmed by coomassie staining. The top panel shows a schematic representation of the modular domain structure of PARN. Ser-557 lies within an optimal MK2 consensus phosphorylation motif located C-terminal to the RNA recognition motif (RRM).

(B) MK2 mediates doxorubicin-induced phosphorylation of PARN on Ser-557 within cells. U2OS cells were infected with lentiviruses expressing luciferase or an MK2-specific shRNA. Following selection, cells were treated with 10 μM doxorubicin for 4 hr and endogenous PARN was affinity purified from cell lysates. The immunoprecipitated material was analyzed by mass spectrometry. (Insets) Only nonphosphorylated Ser-557 PARN peptides (shown in red) could be detected in untreated U2OS cells expressing the luciferase control shRNA (shLuci, co). In contrast, Ser-557-phosphorylated peptides (shown in black) were readily detected when luciferase control cells were exposed to doxorubicin (shLuci, dox). DNA damage-induced phosphorylation of PARN on Ser-557 was completely abolished in MK2-depleted cells (shMK2 co and dox panels).

(C and D) PARN Ser-557 phosphorylation is critical for maintenance of a doxorubicin-induced cell-cycle arrest. HeLa cells were infected with lentiviruses expressing empty transfer vector or PARN shRNA-expressing vectors. PARN shRNA-expressing cells were also cotransfected with shRNA-resistant PARN wild-type or a Ser-557 to Ala mutant. Cells were treated with 0.1 μM doxorubicin for 1 hr, and cell-cycle profiles (phosphohistone H3 and DNA content) were assessed in a nocodazole trap experiment using FACS to monitor mitotic entry and cell-cycle progression. After 24 hr, 5 mM caffeine was added to abrogate checkpoint signaling and analyze the ability of damaged cells to exit the checkpoint. Empty vector, PARN shRNA, and PARN shRNA-expressing cells that were complemented with shRNA-resistant wild-type PARN showed the induction of a stable cell-cycle arrest, as evidenced by an accumulation of S and G$_2$/pHH3-negative cells. PARN shRNA-expressing cells that were coexpressing the shRNA-resistant, nonphosphorylatable PARN S557A mutant failed to maintain a functional cell-cycle arrest, indicated by the accumulation of ~12% of pHH3-positive cells at 24 hr following addition of low-dose doxorubicin. Mean values are shown with error bars indicating standard deviation.

(E) PARN Ser-557 is critical for long-lasting expression of Gadd45α mRNA and protein following doxorubicin-induced genotoxic stress. Cells were transfected and treated with doxorubicin as in (C). Gadd45α mRNA levels were monitored by RT-PCR and protein levels were assessed by immunoblotting. Of note, cells expressing the nonphosphorylatable PARN S557A mutant showed upregulation of Gadd45α mRNA and protein levels at 12 hr, but could not sustain the stabilization of this inherently unstable mRNA for longer times. This loss of Gadd45α expression at 24 hr coincided with the premature cell-cycle checkpoint collapse shown in (C).

Next, to determine whether MK2-dependent phosphorylation of PARN on Ser-557 plays a role in checkpoint control, we used RNAi to deplete endogenous PARN from HeLa cells (Figure S1E) and complemented these cells with RNAi-resistant FLAG-tagged wild-type PARN or with the Ser-557 to Ala PARN mutant. The cells were treated with low-dose (0.1 μM)

doxorubicin for 1 hr, the drug washed out, and the spontaneous escape of cells from the doxorubicin-induced cell-cycle checkpoints monitored 12 and 24 hr later using the nocodazole mitotic-trap assay as in Figure 1. As shown in Figures 6C and 6D, control cells expressing either an empty vector or PARN shRNA mounted and maintained a robust doxorubicin-induced cell-cycle arrest 12 and 24 hr later, indicated by an accumulation of cells with a 4N DNA content that stained largely negative for the mitotic marker pHH3. A similar pattern was observed in PARN-depleted cells that were complemented with exogenous wild-type PARN. In stark contrast, cells depleted of endogenous PARN and complemented with the Ser-557 to Ala mutant could initiate, but were unable to maintain a prolonged doxorubicin-induced cell-cycle arrest, indicated by the accumulation of 11.7% pHH3-positive cells 24 hr after the addition of doxorubicin. As a control, 5 mM caffeine was then added to each of the plates following the 24 hr measurement to inhibit ATM/ATR/DNA-PK and chemically inactivate the DNA damage checkpoint. This resulted in similar checkpoint release from all the PARN-manipulated cells, verifying that the cells after each treatment are equally viable and competent to enter mitosis. These observations demonstrate that phosphorylation of PARN on Ser-557 by MK2 is required for proper cell-cycle checkpoint maintenance, and suggest that phosphorylation of PARN may alter the degradation of specific RNAs involved in checkpoint control.

Finally, to investigate whether the role of MK2-mediated PARN phosphorylation in cell-cycle control was mediated through posttranscriptional control of Gadd45α mRNA, analogous to what we observed for hnRNPA0, we assayed lysates from the PARN-depletion/complementation experiments described above for Gadd45α mRNA levels. In response to doxorubicin, all cells showed robust upregulation of Gadd45α mRNA at 12 hr after treatment (Figure 6E). In PARN-depleted cells complemented with empty vector or wild-type PARN, the elevated levels of Gadd45α mRNA and protein were further maintained for 24 hr, which was the duration of the experiment prior to addition of caffeine. In marked contrast, PARN-depleted cells complemented with the nonphosphorylatable PARN mutant showed a precipitous decline in Gadd45α mRNA levels back to baseline values between 12 and 24 hr, and only a minuscule amount of protein at 24 hr, consistent with the premature checkpoint collapse we had observed earlier. Upon forced cell-cycle re-entry by caffeine addition, Gadd45α mRNA and protein levels dropped below the limits of detection following all of the cell treatments (Figure 6E, 48 hr lanes). Together, these data show that MK2 phosphorylation of PARN on Ser-557 in response to genotoxic stress is critical for maintenance of both Gadd45α mRNA and protein expression in response to DNA damage.

A Gadd45α-Mediated Positive Feedback Loop Is Required for Sustaining Long-Term MK2 Activity to Suppress Cdc25B and C-Driven Mitotic Re-entry after Genotoxic Stress

Members of the Cdc25 family are critical checkpoint kinase substrates for cell-cycle control in response to DNA damage. We and others have provided evidence that the checkpoint func-

tion of MK2 may, at least in part, be mediated through MK2-dependent phosphorylation and cytoplasmic sequestration/inactivation of members of the Cdc25 family (Manke et al., 2005; Lopez-Aviles et al., 2005; Reinhardt et al., 2007). We therefore asked whether the MK2-dependent regulation of Gadd45α that was required for maintenance of late cell-cycle arrest after DNA damage was somehow related to this previously discovered MK2-dependent checkpoint function involving inactivation of Cdc25B and C. Intriguingly in this regard, Gadd45α was previously shown to positively regulate the p38 pathway through a mechanism that is not entirely clear (Bulavin et al., 2003). We therefore postulated that Gadd45α might form part of a positive feedback loop that was required to sustain long-term activation of MK2 through its upstream regulator p38. Initial experiments explored whether Gadd45α physically interacted with known components of the p38 pathway using immunoprecipitation experiments. No direct interactions between HA-tagged Gadd45α and the endogenous kinases MKK3 or -6, two known upstream regulators of p38 that respond to inflammatory stimuli or UV irradiation, could be detected in these experiments (data not shown). However, as shown in Figure 7A, we did observe a strong interaction between Gadd45α and p38 itself. Furthermore, when Gadd45α was depleted using RNAi, as shown in Figures 7B and 7C, there was a loss of p38-dependent MK2 phosphorylation specifically at late times after DNA damage. Importantly, the loss of Gadd45α had little if any effect on MK2 activation at early times. These observations suggest a model in which the initial activation of MK2 after genotoxic stress does not depend on Gadd45α, but subsequent p38/MK2-dependent stabilization of Gadd45α, through phosphorylation of TIAR, PARN, and hnRNPA0, becomes required for maintaining the phosphorylated and active form of MK2 at late times (Figure 7D). If this model of an MK2-driven Gadd45α-positive feedback is correct, and late MK2 activity is itself critical for controlling Cdc25B and C activity and localization, then loss of MK2 would be expected to result in misregulation of Cdc25B/C beginning at around 24 hr (Figure 7B). To investigate this, we examined the subcellular localization of Cdc25B/C, along with phenotypic responses, in cells in which this feedback loop was disrupted (Figure 8). In these experiments, stable cell lines expressing GFP-tagged versions of Cdc25B/C were generated and subsequently infected with lentiviral shRNAs targeting MK2, Chk1, or luciferase (control). The cells were treated with low-dose (0.1 μM) doxorubicin for 30 min and the subcellular localization of CDC25B/C monitored in live cells by time-lapse fluorescence microscopy. As shown in Figures 8A and 8B, in control cells, Cdc25B/C lose their cytoplasmic sequestration and first appear in the nucleus at 30.3 ± 3.9 hr and 30.3 ± 3.7 hr, respectively, after this low-level DNA-damaging treatment. This nuclear entry was followed by a cytologically normal mitotic cell division that occurred ∼2 hr later, producing two intact daughter cells (Figure 8A, top row of upper and lower panels, arrows indicate the two daughter cells). In Chk1-depleted cells, nuclear entry of Cdc25B/C after this treatment occurred much more rapidly, with a mean onset at 15.4 ± 3.9 hr and 15.3 ± 4.5 hr, respectively (Figures 8A and 8C). This premature nuclear entry was invariably followed by catastrophic mitosis resulting in apoptosis, indicated by prominent
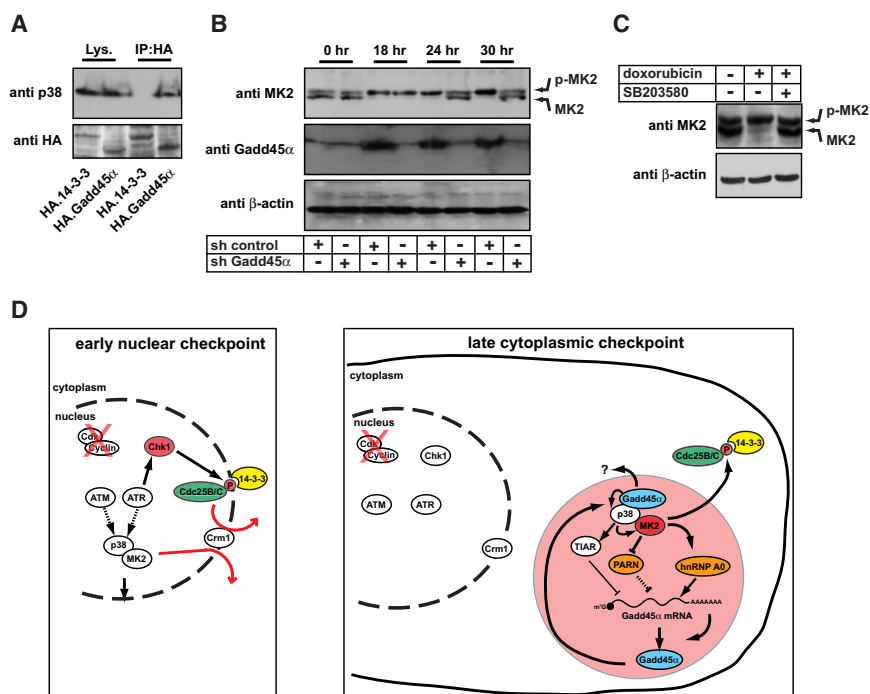
Figure 7. Gadd45α Is Required to Maintain Long-Term MK2 Activity and Prevent Premature Checkpoint Collapse following Genotoxic Stress

(A) Gadd45α interacts with p38. Cells were transfected with HA-tagged Gadd45α or HA-tagged 14-3-3ζ as a negative control. Lysates and anti-HA IPs were analyzed by SDS-PAGE and western blotting using anti-p38 and anti-HA-antibodies.

(B) Gadd45α is required to maintain long-term MK2 activity following doxorubicin-induced DNA damage. HeLa cells were infected with lentiviruses expressing either luciferase control shRNA or MK2-specific hairpins, treated with 1 μM doxorubicin for the indicated times, lysed, and proteins separated on SDS-PAGE. MK2 and Gadd45α levels were monitored by immunoblot; β-actin staining served as a loading control. Both Gadd45α and control shRNA-expressing cells showed a robust induction of MK2 activity 18 hr following doxorubicin treatment (monitored by phosphorylation-induced gel shift to a slower-migrating isoform on SDS-PAGE). However, control cells maintained MK2 activity for at least 30 hr, while Gadd45α-depleted cells were unable to maintain MK2 activity for more than 18 hr.

(C) The activation-induced MK2 gel shift is blocked by the p38 inhibitor SB203580. Doxorubicin treatment (10 μM) of HeLa cells induces a phosphoryla-tion-dependent gel shift of MK2 (middle lane). Pretreatment of HeLa cells with 10 μM of the p38 inhibitor SB203580 abolished the activation-induced MK2 gel shift (right lane).

(D) A simplified model depicting the early, Chk1-dependent nuclear checkpoint (left box) and the late MK2-dependent cytoplasmic checkpoint (right box). Dashed arrows between ATM/ATR and p38/MK2 indicate intermediate steps that are not shown. The MK2-mediated cytoplasmic checkpoint is sustained through a positive feedback loop. Following nuclear activation, the p38/MK2 signaling complex relocalizes to the cytoplasm through a Crm1-dependent transport mechanism. MK2-mediated hnRNPA0 and PARN phosphorylation, as well as p38-dependent TIAR phosphorylation, are required to stabilize Gadd45α mRNA, resulting in increased Gadd45α protein levels. Gadd45α itself is then required to maintain MK2 activity in the cytoplasm.

membrane blebbing and nuclear pyknosis and disintegration (Figure 8B and data not shown). In contrast, in MK2-depleted cells, nuclear entry of Cdc25B/C was delayed relative to Chk1-depleted cells, but occurred significantly earlier than in control cells, with a mean appearance time of 23.9 ± 6.0 hr and 22.4 ± 4.1 hr, respectively (Figures 8A and 8C). Intriguingly, this time corresponds exactly to the time when MK2 activity declines in the absence of Gadd45α (Figure 7B), strongly implying that the positive feedback loop involving MK2-dependent stabilization of Gadd45α, followed by Gadd45α-dependent sustainment of MK2 activity, is critical for prolonged Cdc25 inhibition and maintenance of a G_2 arrest. Together, these data suggest that the p38 → MK2 → Gadd45α → p38 positive feedback loop is essential to allow cells to recover from the doxorubicin-induced DNA damage before committing to the next mitotic cell division.

DISCUSSION

The DNA Damage Response Regulates Cytoplasmic Proteins that Modulate mRNA Stability

In this manuscript we have identified a critical role for cytoplasmic MK2 activity in regulating the G_2/M transition of p53-defective cells after DNA damage by posttranscriptional regulation of proteins involved in RNA regulation. In contrast to transcriptional control, the general importance of posttranscriptional and translational regulatory circuits in regulating gene expression in a wide variety of biological contexts is only now becoming increasingly recognized. In this regard we note that the largest subset of ATM/ATR/DNA-PK substrates identified in a recent phosphoproteomic screen were proteins linked to RNA and DNA metabolism, particularly those proteins involved in posttranscriptional mRNA regulation (Matsuoka et al., 2007). Likewise, a genome-wide siRNA screen looking for modulators of DNA damage signaling similarly revealed that the largest number of "hits" were those targeting gene products responsible for nucleic acid metabolism, particularly those involved in mRNA binding and processing (Paulsen et al., 2009). Those convergent observations, from two very different experimental approaches, highlight the potential emerging importance of regulatory circuits controlling RNA metabolism and stability in DNA repair and checkpoint function, and strongly argue that the DNA damage response may extend substantially beyond the canonical ATM/Chk2 and ATR/Chk1 signaling cascades that have been described to date. Our findings implicating MK2 in regulation of mRNA stabilization through modification of hnRNPA0 and PARN lend support to this concept.

Premature Mitotic Entry following DNA Damage in p53-Deficient Cells Is Prevented by Two Temporally and Spatially Distinct Checkpoint Networks

In resting cells, MK2 is localized in the nucleus, as part of a tight complex with its upstream activating kinase p38. Chemical
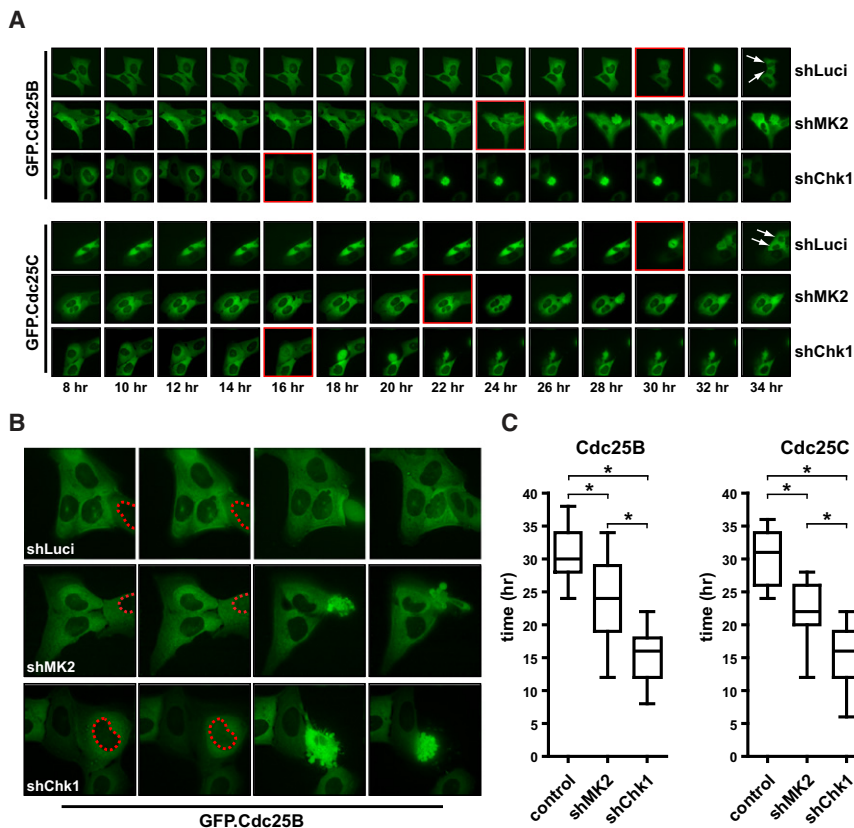
Figure 8. MK2 Is Required for the Retention of Cdc25B and -C in the Cytoplasm at Late Stages of the Cell-Cycle Checkpoint Response to Prevent Inappropriate Mitotic Re-entry

(A) HeLa cells were infected with retroviruses encoding GFP-fused Cdc25B (upper panels) or Cdc25C (lower panels). GFP.Cdc25B/C-expressing cells were subsequently infected with lentiviruses expressing luciferase-, MK2-, or Chk1-specific shRNA; treated with 0.1 μM doxorubicin for 30 min; and GFP localization monitored by live-cell imaging. Control cells mounted a cell-cycle checkpoint response and resumed mitotic cell division after ~30 hr with the production of two intact daughter cells (top panels and top panel in (B). MK2-depleted cells initiated a checkpoint response, which collapsed after ~24 hr invariably followed by a catastrophic mitotic event (middle panels and B, middle panel). Chk1-depleted cells entered a premature, catastrophic mitotic event at ~16 hr following doxorubicin (middle panels and B, middle panel) Red frames indicate the time at which nuclear relocalization of Cdc25B/C could first be observed.

(B) Detailed view of the mitotic events in the three different GFP.Cdc25B-labeled cell lines. Red dashed line highlights the nuclear border.

(C) Quantitative analysis of the data shown in (A) and (B). Data are shown as box and whisker plots and represent 18 independent experiments for each cell line. The time of the first appearance of a mitotic figure was recorded. Asterisk indicates statistical significance. Mean values are shown as lines within boxes indicating 25th and 75th percentiles. Whiskers show maximal and minimal values observed.

stressors, such as arsenite and anisomycin, have been shown to induce the cytoplasmic translocation of p38:MK2 complexes (Ben-Levy et al., 1998; Engel et al., 1998), where MK2 acts as a "molecular chauffer" with p38-dependent phosphorylation of MK2 revealing Crm1-recognizable NES sequences (Meng et al., 2002; ter Haar et al., 2007). Our findings now extend this dynamic, phospho-dependent relocalization of MK2 in the context of genotoxic stress.

In contrast to the cytoplasmic localization of active MK2, Chk1 has been reported to be largely nuclear following DNA damage-induced activation (Jiang et al., 2003; Sanchez et al., 1997), although some localization of Chk1 to the centrosome has been described (Kramer et al., 2004). While a component of MK2 activity may similarly reside at the centrosome, we observed that the bulk of MK2 appears to be diffusely localized throughout the cytoplasm. Furthermore, the discrepancy in time between the "early" loss of the G_2/M checkpoint following knockdown of Chk1 and the "late" loss of the checkpoint upon loss of MK2 lends additional support to a model in which Chk1 and MK2 control spatially and temporally distinct substrate pools (c.f. Figure 7D).

RNA-Binding and Processing Proteins as Key Targets of Protein Kinase Signaling Pathways

One major function of MK2 is the posttranscriptional regulation of unstable inflammatory cytokine mRNAs such as TNFα, MIP-2, IL-6, and IL-1α, particularly in response to neutrophil and macrophage activation by various stimuli such as LPS (Gaestel, 2006; Janes et al., 2008; Rousseau et al., 2002). Many of these unstable mRNAs contain 3′UTRs carrying AREs with an AUUUA consensus motif (Barreau et al., 2005), and are known to interact with RBPs. Some ARE-binding RBPs, such as TTP, KSRP, AUF1, and BRF1, have been shown to mediate mRNA decay, while other ARE-binding RBPs, such as hnRNPA0, increase the stability of ARE-containing mRNAs (Dean et al., 2004). Furthermore, ARE-binding RBPs such as TIA-1 and TIAR appear to control the translation of their client mRNAs, while HuR and Hu-related proteins control both mRNA turnover and translatability (Dean et al., 2004). RBP binding to ARE mRNA is a highly sequence-specific process that has classically been thought to depend primarily on the affinity of the RBP for particular mRNA sequences. Our findings indicate that phosphorylation of RBPs by kinases such as MK2 and p38 is likely to be a key regulatory mechanism that controls specific RBP:mRNA interactions relevant to cell-cycle control in cancer cells (Figure 5). Similar kinase-dependent interactions have recently been shown for the RBP HuR and the protein kinases Chk2 and p38 (Abdelmohsen et al., 2007; Lafarga et al., 2009). Furthermore, the observation that a sizeable number of RNA-interacting molecules were also putative targets of ATM/ATR/DNA-PK based on mass spectrometry-driven phosphoproteomics (Matsuoka et al., 2007) suggests that this phenomenon may have a more general role in regulating the DNA damage response.

A key unstable mRNA whose levels increased in an MK2-dependent manner after DNA damage was Gadd45α, which is intimately involved in the DNA damage response through mechanisms that remain incompletely understood. Gadd45α is induced both in a p53-dependent and -independent manner, in response to genotoxic stress (Fornace et al., 1989; Kastan et al., 1992). Gadd45α induction in p53-defective cells is mediated in part through the transcription factors ATF2 (a known p38 target), Oct-1, BRCA1, NF-I, and NF-YA (Jin et al., 2001; Maekawa et al., 2008). In addition, there appears to be another layer of control in Gadd45α mRNA expression mediated by alterations in its posttranscriptional stability. An elegant recent study by Gorospe and colleagues showed that Gadd45α transcripts were highly unstable in resting cells (Lal et al., 2006). This rapid degradation under non-stress conditions was mediated, in part, through association of the transcript with AUF1, a protein known to be involved in mRNA decay. Additionally, the translational inhibitor TIAR has been shown to complex with Gadd45α mRNA, ultimately resulting in repression of Gadd45α protein expression (Lal et al., 2006). Upon exposure to the alkylating agent MMS, both AUF1 and TIAR dissociated from the Gadd45α mRNA, allowing for stabilization of the transcript and protein induction. Interestingly, these observations were made in functionally p53-deficient HeLa cells, supporting the importance of posttranscriptional control in this setting. Our results further extend the mechanism of Gadd45α control through p38-mediated phosphorylation of TIAR, resulting in dissociation of the TIAR:Gadd45α RNP complex, and MK2-mediated phosphorylation of both hnRNPA0, and PARN, leading to enhanced Gadd45α mRNA:hnRNPA0 interaction and stability, and increased levels of Gadd45α protein.

Gadd45α Is Part of a Positive Feedback Loop that Suppresses Premature Mitotic Entry

Gadd45α belongs to a family of stress-responsive genes that are induced following DNA damage. Intriguingly, $Gadd45\alpha^{-/-}$ cells have been shown to display a high degree of genomic instability, and $Gadd45\alpha^{-/-}$ mice show increased radiation-induced carcinogenesis (Hollander et al., 1999; Zhan et al., 1999). Gadd45α has been proposed to function at the molecular level through a variety of mechanisms, including binding to MTK1/MEKK4 (Miyake et al., 2007; Takekawa and Saito, 1998), p38 (Bulavin et al., 2003), DNA demethylation (Barreto et al., 2007), and competing for cyclin B binding to Cdk1 (Zhan et al., 1999). In our hands, we were unable to recapitulate this latter effect, and addition of recombinant Gadd45α had no effect on the kinase activity of purified CyclinB/Cdk1 in vitro (D. Lim and M.B.Y., unpublished data). Instead, we observed a robust interaction between Gadd45α and p38 together with a marked loss of p38-mediated MK2 activation, only at late times, in cells lacking Gadd45α. These data suggest a positive feedback model for checkpoint maintenance mediated through late cytoplasmic checkpoint kinase activity and posttranscriptional mRNA stabilization (Figure 7D). At the systems level, positive feedback circuits have been shown to be important for the irreversible reinforcement of critical cellular decision processes, including apoptosis, mitotic entry, R-point transition, and cell-cycle restart following recovery from genotoxic injury. Our findings now

demonstrate that a topologically similar positive feedback loop involving the interplay between protein kinase signal transduction pathways and control of gene expression at the posttranscriptional level is essential for maintenance of prolonged cell-cycle arrest after DNA damage.

EXPERIMENTAL PROCEDURES

Live-Cell Imaging

For live-cell imaging, cells were grown on four chambered glass-bottom slides from Nunc. Images were obtained using a DeltaVision Core live-cell microscopy imaging system maintained at 37°C and 5% CO_2 (Applied Precision) and equipped with a Coolsnap CCD camera. Improvision deconvolution and softWoRx software packages were used for image analysis.

RNA Immunoprecipitation

Cells were lysed in 0.5 ml of ice-cold RNA lysis buffer (110 mM CH_3COOK, 2 mM $Mg[CH_3COO]_2$, 10 mM HEPES [pH 7.4], 200 mM KCl, 0.5% NP-40, 40 μl/ml complete protease inhibitor [Roche], and 50 units/ml RNAsin) per 10 cm dish on ice. Extracts were homogenized using a 26.5 gauge needle, cleared by centrifugation at 4200 rpm for 10 min and incubated with antibody-coated beads for 2 hr. After extensive washing in TBS, beads were eluted with 0.5 ml elution buffer (10 mM Tris-HCl [pH 7.5], 1 mM EDTA, 1% SDS, Proteinase K) for 1 hr at 37°C with rocking. Eluted material was phenol/chloroform extracted followed by CH_3COONH_4/isopropanol precipitation. Pellets were washed in 70% ethanol, resuspended in H_2O, and DNase treated, and reverse transcribed using MMLV RT (Ambion) with random hexamer primers. Primers for the subsequent PCR were as follows: 5′-GAT GCCCTGGAGGAAGTGCT-3′ (forward) and 5′-AGCAGGCACAACACCACG TT-3′ (reverse) for Gadd45α and 5′-TGCACCACCAACTGCTTAGC-3′ (forward) and 5′-GGCATGGACTGTGGTCATGAG-3′ (reverse) for GAPDH amplification (Lal et al., 2006).

Additional details and methods are described in the Supplemental Information.

SUPPLEMENTAL INFORMATION

Supplemental Information includes four figures and Supplemental Experimental Procedures and can be found with this article online at doi:10.1016/j.molcel.2010.09.018.

REFERENCES

Abdelmohsen, K., Pullmann, R., Jr., Lal, A., Kim, H.H., Galban, S., Yang, X., Blethrow, J.D., Walker, M., Shubert, J., Gillespie, D.A., et al. (2007). Phosphorylation of HuR by Chk2 regulates SIRT1 expression. Mol. Cell 25, 543–557.

Abraham, R.T. (2001). Cell cycle checkpoint signaling through the ATM and ATR kinases. Genes Dev. *15*, 2177–2196.

Anderson, P., and Kedersha, N. (2002). Stressful initiations. J. Cell Sci. *115*, 3227–3234.

Barreau, C., Paillard, L., and Osborne, H.B. (2005). AU-rich elements and associated factors: are there unifying principles? Nucleic Acids Res. *33*, 7138–7150.

Barreto, G., Schafer, A., Marhold, J., Stach, D., Swaminathan, S.K., Handa, V., Doderlein, G., Maltry, N., Wu, W., Lyko, F., and Niehrs, C. (2007). Gadd45a promotes epigenetic gene activation by repair-mediated DNA demethylation. Nature *445*, 671–675.

Bartek, J., and Lukas, J. (2003). Chk1 and Chk2 kinases in checkpoint control and cancer. Cancer Cell *3*, 421–429.

Bartkova, J., Rezaei, N., Liontos, M., Karakaidos, P., Kletsas, D., Issaeva, N., Vassiliou, L.V., Kolettas, E., Niforou, K., Zoumpourlis, V.C., et al. (2006). Oncogene-induced senescence is part of the tumorigenesis barrier imposed by DNA damage checkpoints. Nature *444*, 633–637.

Ben-Levy, R., Hooper, S., Wilson, R., Paterson, H.F., and Marshall, C.J. (1998). Nuclear export of the stress-activated protein kinase p38 mediated by its substrate MAPKAP kinase-2. Curr. Biol. *8*, 1049–1057.

Boutros, R., Lobjois, V., and Ducommun, B. (2007). CDC25 phosphatases in cancer cells: key players? Good targets? Nat. Rev. Cancer *7*, 495–507.

Bulavin, D.V., Higashimoto, Y., Popoff, I.J., Gaarde, W.A., Basrur, V., Potapova, O., Appella, E., and Fornace, A.J., Jr. (2001). Initiation of a G2/M checkpoint after ultraviolet radiation requires p38 kinase. Nature *411*, 102–107.

Bulavin, D.V., Kovalsky, O., Hollander, M.C., and Fornace, A.J., Jr. (2003). Loss of oncogenic H-ras-induced cell cycle arrest and p38 mitogen-activated protein kinase activation by disruption of Gadd45a. Mol. Cell. Biol. *23*, 3859–3871.

Chen, Z., Xiao, Z., Gu, W.Z., Xue, J., Bui, M.H., Kovar, P., Li, G., Wang, G., Tao, Z.F., Tong, Y., et al. (2006). Selective Chk1 inhibitors differentially sensitize p53-deficient cancer cells to cancer therapeutics. Int. J. Cancer *119*, 2784–2794.

Dean, J.L., Sully, G., Clark, A.R., and Saklatvala, J. (2004). The involvement of AU-rich element-binding proteins in p38 mitogen-activated protein kinase pathway-mediated mRNA stabilisation. Cell. Signal. *16*, 1113–1121.

Di Micco, R., Fumagalli, M., Cicalese, A., Piccinin, S., Gasparini, P., Luise, C., Schurra, C., Garre, M., Nuciforo, P.G., Bensimon, A., et al. (2006). Oncogene-induced senescence is a DNA damage response triggered by DNA hyper-replication. Nature *444*, 638–642.

Donzelli, M., and Draetta, G.F. (2003). Regulating mammalian checkpoints through Cdc25 inactivation. EMBO Rep. *4*, 671–677.

Engel, K., Kotlyarov, A., and Gaestel, M. (1998). Leptomycin B-sensitive nuclear export of MAPKAP kinase 2 is regulated by phosphorylation. EMBO J. *17*, 3363–3371.

Fornace, A.J., Jr., Nebert, D.W., Hollander, M.C., Luethy, J.D., Papathanasiou, M., Fargnoli, J., and Holbrook, N.J. (1989). Mammalian genes coordinately regulated by growth arrest signals and DNA-damaging agents. Mol. Cell. Biol. *9*, 4196–4203.

Gaestel, M. (2006). MAPKAP kinases—MKs—two's company, three's a crowd. Nat. Rev. Mol. Cell Biol. *7*, 120–130.

Harkin, D.P., Bean, J.M., Miklos, D., Song, Y.H., Truong, V.B., Englert, C., Christians, F.C., Ellisen, L.W., Maheswaran, S., Oliner, J.D., and Haber, D.A. (1999). Induction of GADD45 and JNK/SAPK-dependent apoptosis following inducible expression of BRCA1. Cell *97*, 575–586.

Harper, J.W., and Elledge, S.J. (2007). The DNA damage response: ten years after. Mol. Cell *28*, 739–745.

Hollander, M.C., Sheikh, M.S., Bulavin, D.V., Lundgren, K., Augeri-Henmueller, L., Shehee, R., Molinaro, T.A., Kim, K.E., Tolosa, E., Ashwell, J.D., et al. (1999). Genomic instability in Gadd45a-deficient mice. Nat. Genet. *23*, 176–184.

Jackson, S.P., and Bartek, J. (2009). The DNA-damage response in human biology and disease. Nature *461*, 1071–1078.

Janes, K.A., Reinhardt, H.C., and Yaffe, M.B. (2008). Cytokine-induced signaling networks prioritize dynamic range over signal strength. Cell *135*, 343–354.

Jiang, K., Pereira, E., Maxfield, M., Russell, B., Goudelock, D.M., and Sanchez, Y. (2003). Regulation of Chk1 includes chromatin association and 14-3-3 binding following phosphorylation on Ser-345. J. Biol. Chem. *278*, 25207–25217.

Jin, S., Fan, F., Fan, W., Zhao, H., Tong, T., Blanck, P., Alomo, I., Rajasekaran, B., and Zhan, Q. (2001). Transcription factors Oct-1 and NF-YA regulate the p53-independent induction of the GADD45 following DNA damage. Oncogene *20*, 2683–2690.

Kastan, M.B., and Bartek, J. (2004). Cell-cycle checkpoints and cancer. Nature *432*, 316–323.

Kastan, M.B., Zhan, Q., el-Deiry, W.S., Carrier, F., Jacks, T., Walsh, W.V., Plunkett, B.S., Vogelstein, B., and Fornace, A.J., Jr. (1992). A mammalian cell cycle checkpoint pathway utilizing p53 and GADD45 is defective in ataxia-telangiectasia. Cell *71*, 587–597.

Koniaras, K., Cuddihy, A.R., Christopoulos, H., Hogg, A., and O'Connell, M.J. (2001). Inhibition of Chk1-dependent G2 DNA damage checkpoint radiosensitizes p53 mutant human cells. Oncogene *20*, 7453–7463.

Kramer, A., Mailand, N., Lukas, C., Syljuasen, R.G., Wilkinson, C.J., Nigg, E.A., Bartek, J., and Lukas, J. (2004). Centrosome-associated Chk1 prevents premature activation of cyclin-B-Cdk1 kinase. Nat. Cell Biol. *6*, 884–891.

Kyriakis, J.M., and Avruch, J. (2001). Mammalian mitogen-activated protein kinase signal transduction pathways activated by stress and inflammation. Physiol. Rev. *81*, 807–869.

Lafarga, V., Cuadrado, A., Lopez de Silanes, I., Bengoechea, R., Fernandez-Capetillo, O., and Nebreda, A.R. (2009). p38 Mitogen-activated protein kinase- and HuR-dependent stabilization of p21(Cip1) mRNA mediates the G(1)/S checkpoint. Mol. Cell. Biol. *29*, 4341–4351.

Lal, A., Abdelmohsen, K., Pullmann, R., Kawai, T., Galban, S., Yang, X., Brewer, G., and Gorospe, M. (2006). Posttranscriptional derepression of GADD45alpha by genotoxic stress. Mol. Cell *22*, 117–128.

Linding, R., Jensen, L.J., Ostheimer, G.J., van Vugt, M.A., Jorgensen, C., Miron, I.M., Diella, F., Colwill, K., Taylor, L., Elder, K., et al. (2007). Systematic discovery of in vivo phosphorylation networks. Cell *129*, 1415–1426.

Lopez-Aviles, S., Grande, M., Gonzalez, M., Helgesen, A.L., Alemany, V., Sanchez-Piris, M., Bachs, O., Millar, J.B., and Aligue, R. (2005). Inactivation of the Cdc25 phosphatase by the stress-activated Srk1 kinase in fission yeast. Mol. Cell *17*, 49–59.

Maekawa, T., Sano, Y., Shinagawa, T., Rahman, Z., Sakuma, T., Nomura, S., Licht, J.D., and Ishii, S. (2008). ATF-2 controls transcription of Maspin and GADD45 alpha genes independently from p53 to suppress mammary tumors. Oncogene *27*, 1045–1054.

Manke, I.A., Nguyen, A., Lim, D., Stewart, M.Q., Elia, A.E., and Yaffe, M.B. (2005). MAPKAP kinase-2 is a cell cycle checkpoint kinase that regulates the G2/M transition and S phase progression in response to UV irradiation. Mol. Cell *17*, 37–48.

Matsuoka, S., Ballif, B.A., Smogorzewska, A., McDonald, E.R., 3rd, Hurov, K.E., Luo, J., Bakalarski, C.E., Zhao, Z., Solimini, N., Lerenthal, Y., et al. (2007). ATM and ATR substrate analysis reveals extensive protein networks responsive to DNA damage. Science *316*, 1160–1166.

Meng, W., Swenson, L.L., Fitzgibbon, M.J., Hayakawa, K., Ter Haar, E., Behrens, A.E., Fulghum, J.R., and Lippke, J.A. (2002). Structure of mitogen-activated protein kinase-activated protein (MAPKAP) kinase 2 suggests a bifunctional switch that couples kinase activation with nuclear export. J. Biol. Chem. *277*, 37401–37405.

Miyake, Z., Takekawa, M., Ge, Q., and Saito, H. (2007). Activation of MTK1/MEKK4 by GADD45 through induced N-C dissociation and dimerization-mediated trans autophosphorylation of the MTK1 kinase domain. Mol. Cell. Biol. *27*, 2765–2776.

Mukhopadhyay, U.K., Senderowicz, A.M., and Ferbeyre, G. (2005). RNA silencing of checkpoint regulators sensitizes p53-defective prostate cancer cells to chemotherapy while sparing normal cells. Cancer Res. 65, 2872–2881.

Neininger, A., Kontoyiannis, D., Kotlyarov, A., Winzen, R., Eckert, R., Volk, H.D., Holtmann, H., Kollias, G., and Gaestel, M. (2002). MK2 targets AU-rich elements and regulates biosynthesis of tumor necrosis factor and inter-leukin-6 independently at different post-transcriptional levels. J. Biol. Chem. 277, 3065–3068.

Obenauer, J.C., Cantley, L.C., and Yaffe, M.B. (2003). Scansite 2.0: proteome-wide prediction of cell signaling interactions using short sequence motifs. Nucleic Acids Res. 31, 3635–3641.

O'Neill, T., Giarratani, L., Chen, P., Iyer, L., Lee, C.H., Bobiak, M., Kanai, F., Zhou, B.B., Chung, J.H., and Rathbun, G.A. (2002). Determination of substrate motifs for human Chk1 and hCds1/Chk2 by the oriented peptide library approach. J. Biol. Chem. 277, 16102–16115.

Paulsen, R.D., Soni, D.V., Wollman, R., Hahn, A.T., Yee, M.C., Guan, A., Hesley, J.A., Miller, S.C., Cromwell, E.F., Solow-Cordero, D.E., et al. (2009). A genome-wide siRNA screen reveals diverse cellular processes and path-ways that mediate genome stability. Mol. Cell 35, 228–239.

Raman, M., Earnest, S., Zhang, K., Zhao, Y., and Cobb, M.H. (2007). TAO kinases mediate activation of p38 in response to DNA damage. EMBO J. 26, 2005–2014.

Reinhardt, H.C., Aslanian, A.S., Lees, J.A., and Yaffe, M.B. (2007). p53-defi-cient cells rely on ATM- and ATR-mediated checkpoint signaling through the p38MAPK/MK2 pathway for survival after DNA damage. Cancer Cell 11, 175–189.

Reinhardt, H.C., and Yaffe, M.B. (2009). Kinases that control the cell cycle in response to DNA damage: Chk1, Chk2, and MK2. Curr. Opin. Cell Biol. 21, 245–255.

Rousseau, S., Morrice, N., Peggie, M., Campbell, D.G., Gaestel, M., and Cohen, P. (2002). Inhibition of SAPK2a/p38 prevents hnRNP A0 phosphoryla-tion by MAPKAP-K2 and its interaction with cytokine mRNAs. EMBO J. 21, 6505–6514.

Sanchez, Y., Wong, C., Thoma, R.S., Richman, R., Wu, Z., Piwnica-Worms, H., and Elledge, S.J. (1997). Conservation of the Chk1 checkpoint pathway in mammals: linkage of DNA damage to Cdk regulation through Cdc25. Science 277, 1497–1501.

Shiloh, Y. (2003). ATM and related protein kinases: safeguarding genome integrity. Nat. Rev. Cancer 3, 155–168.

Takekawa, M., and Saito, H. (1998). A family of stress-inducible GADD45-like proteins mediate activation of the stress-responsive MTK1/MEKK4 MAPKKK. Cell 95, 521–530.

ter Haar, E., Prabhakar, P., Liu, X., and Lepre, C. (2007). Crystal structure of the p38 alpha-MAPKAP kinase 2 heterodimer. J. Biol. Chem. 282, 9733–9739.

Zhan, Q., Antinore, M.J., Wang, X.W., Carrier, F., Smith, M.L., Harris, C.C., and Fornace, A.J., Jr. (1999). Association with Cdc2 and inhibition of Cdc2/Cyclin B1 kinase activity by the p53-regulated protein Gadd45. Oncogene 18, 2892–2900.

Supplemental Information

DNA Damage Activates a Spatially Distinct Late Cytoplasmic Cell-Cycle Checkpoint Network Controlled by MK2-Mediated RNA Stabilization

H. Christian Reinhardt, Pia Hasskamp, Ingolf Schmedding, Sandra Morandell, Marcel A.T.M. van Vugt, XiaoZhe Wang, Rune Linding, Shao-En Ong, David Weaver, Steven A. Carr, and Michael B. Yaffe

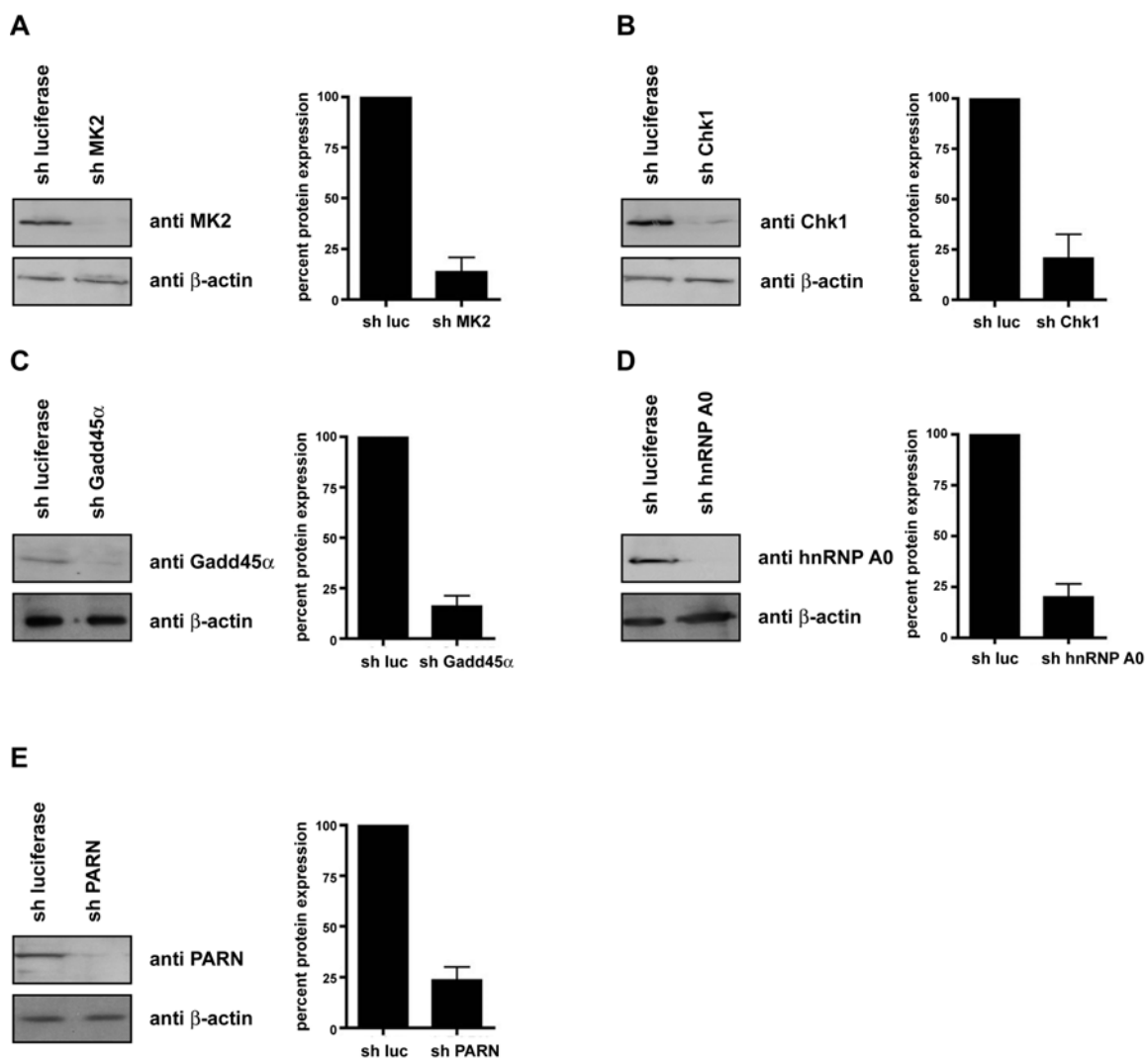### Supplemental Information Inventory

Supplemental Figures
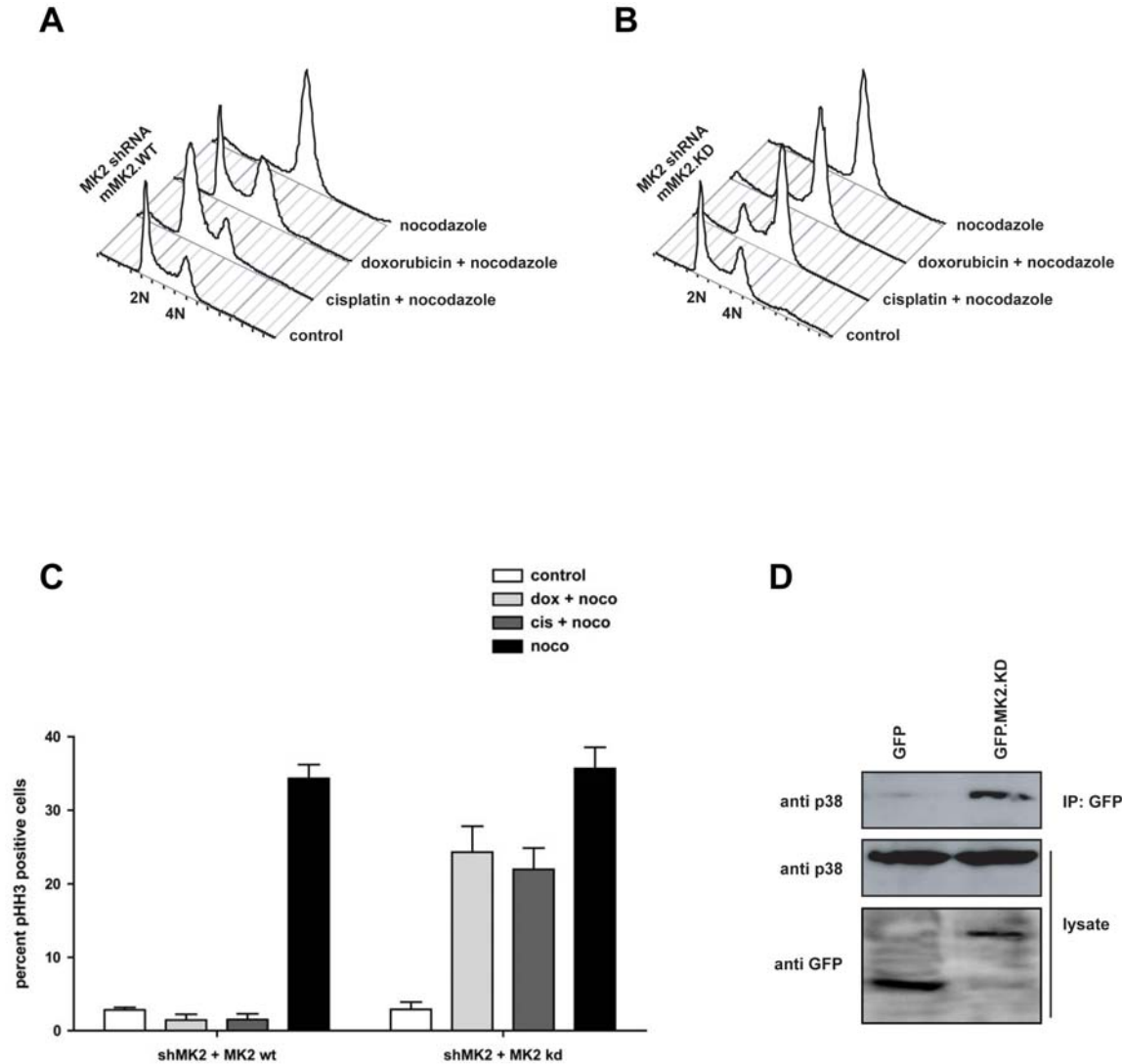
Figure S1

A

B

C

D

E

Figure S1. RNAi-mediated knockdown efficiency.

Cells were infected with lentiviruses expressing shRNAs targeting (**A**) MK2; (**B**) Chk1; (**C**) hnRNP A0; (**D**) Gadd45a or (**E**) PARN. Target cells were incubated with viral supernatants for 24 hr in the presence of 8μM polybrene. After three cycles of infection, cells were selected in puromycin for 48 hr before lysis and assessment of knockdown efficiency by SDS-PAGE. Knockdown efficiency was quantified in separate immunoblots from 3 independent experiments and normalized to β-actin expression using ImageQuant software. Mean values and standard deviations are shown. Panels A and B were performed in U2OS cells, panels C-E were performed in HeLa cells.
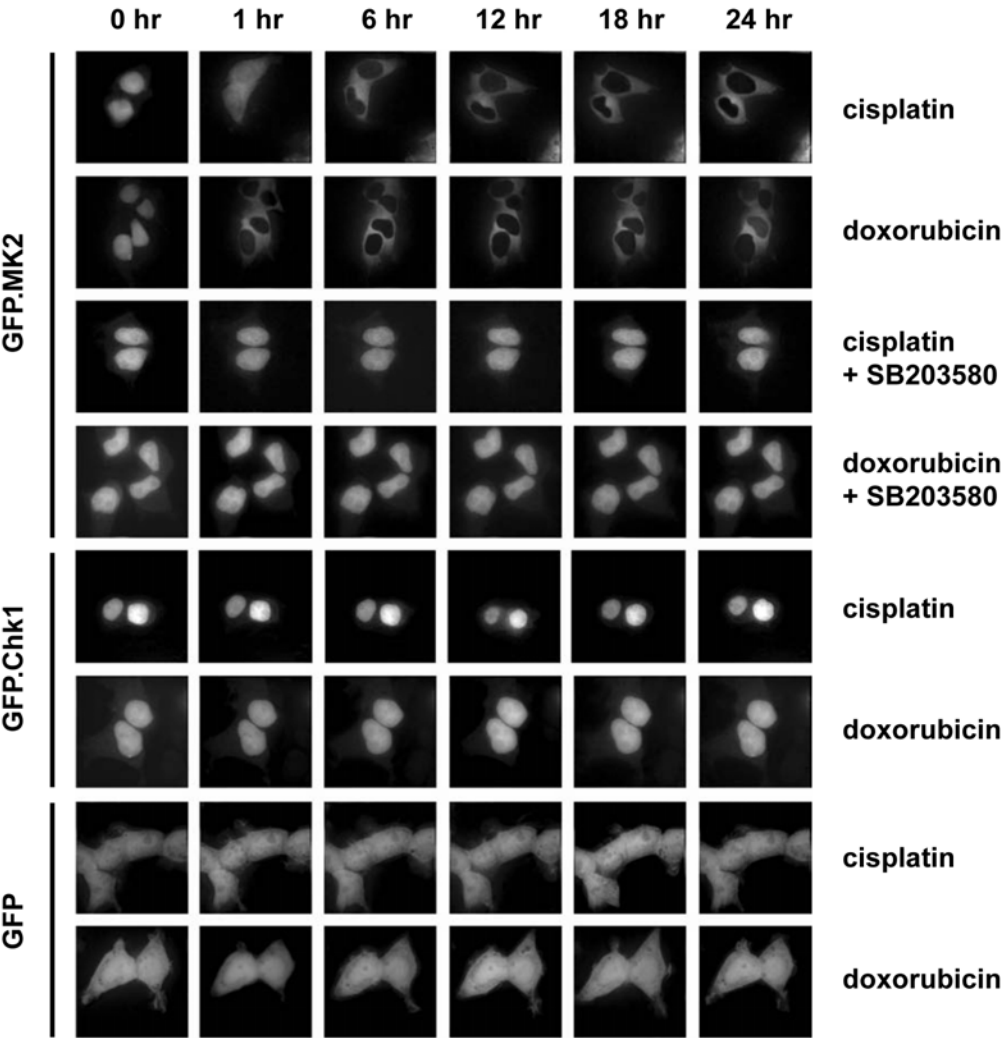
Figure S2

Figure S2. MK2 activity is essential to maintain a prolonged cell cycle arrest following DNA damage.

(A, B) Human U2OS cells were depleted of MK2 using shRNA, and complemented with either shRNA-resistant wildtype murine MK2 (panel A) or a kinase-dead isoform (panel B). Cells were either left untreated (control) or treated with 10 μM of the indicated DNA damaging agents in a 30 hr nocodazole trap experiment,and analysed by flow cytometry. Cells that were complemented with wildtype MK2 were checkpoint competent, while cells that were complemented with the kinase-dead mutant were unable to maintain a functional cell cycle checkpoint as revealed by the accumulation of cells containing 4N DNA content.

(C) Quantification of the mitotic pHH3 staining of the samples shown in panels **A** and **B** (n=6 independent experiments. Mean values and standard deviations are shown.).

(D) Kinase-dead MK2 interacts with p38. Exogenous GFP-tagged kinase-dead MK2 was immunoprecipitated using anti-GFP antibodies. The immunoprecipitated material was resolved on SDS-PAGE gels, and immunoblotted using anti-p38 antibodies. Immunoprecipittaion of exogenous GFP served as a control. A strong interaction between GFP.MK2.kd and endogenous p38 could be detected, while no interaction was seen between the GFP control and p38.
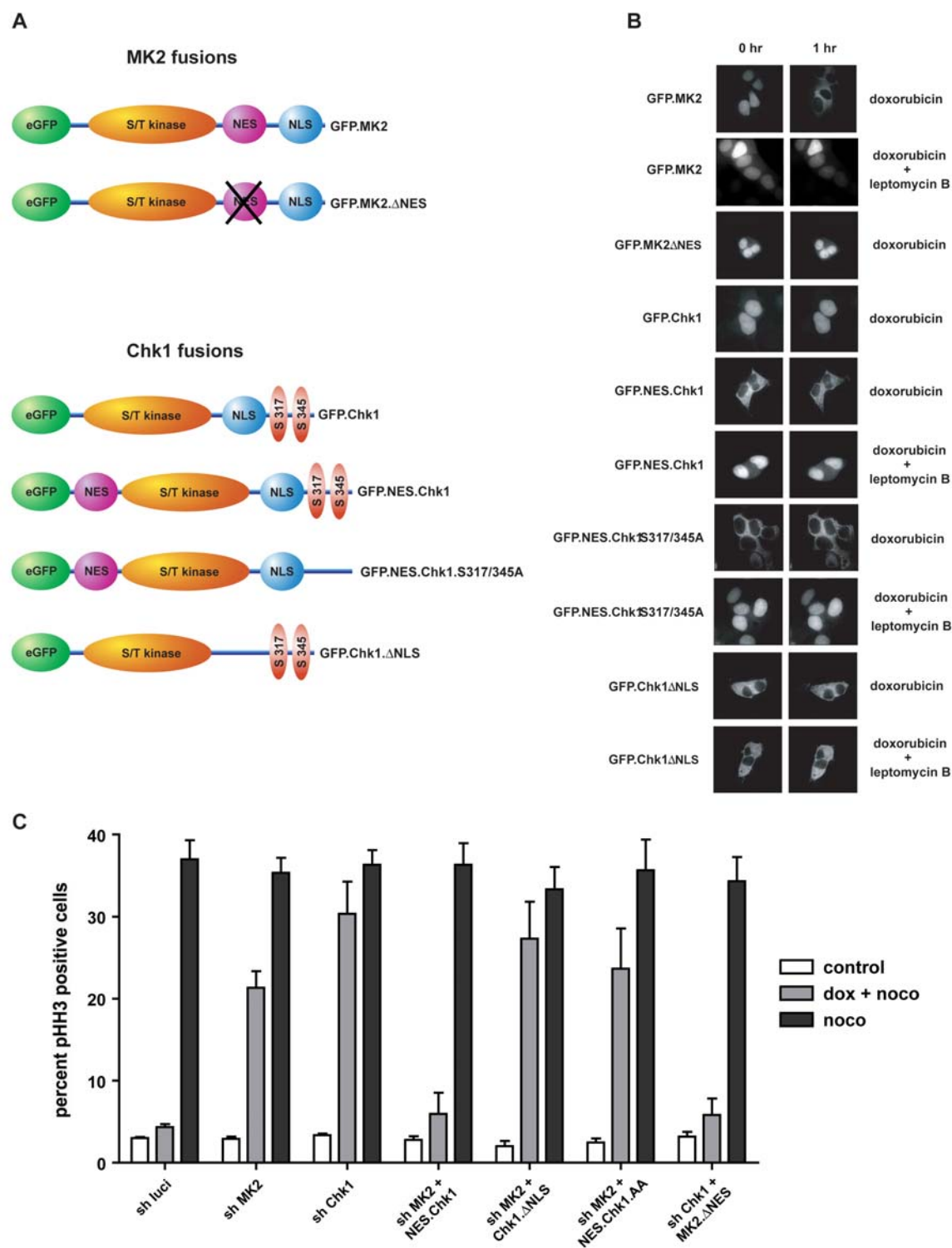
Figure S3

Figure S3. MK2 undergoes p38MAPK- and Crm1-dependent translocation from the nucleus to the cytoplasm in response to genotoxic agents, while Chk1 remains in the nucleus.

GFP.MK2 (top panels) and GFP.Chk1 (middle panels) fusion proteins were stably expressed at low levels in U2OS cells and their dynamic localization in response to the indicated treatments was analyzed at various times using live cell imaging as in Fig. 2. Unfused GFP served as a control (bottom panels). Treatment with 10 μM cisplatin and doxorubicin induced a rapid relocalization of MK2 from the nucleus to the cytoplasm. This re-localization was completely abolished in the presence of 10 μM of the p38 inhibitor SB203580. Chk1 remained predominantly nuclear following treatment with cisplatin or doxorubicin. Unfused GFP was dispersed throughout the nucleus and the cytoplasm and no obvious shifts in this localization pattern were seen following treatment with cisplatin or doxorubicin.

Figure S4

Figure S4. Nuclear and basophilic kinase activities are required for a functional cell cycle checkpoint response.

(A) Structural representation of the modular domain organization of the localization and kinase activation mutants that were used.

(B) Localization patterns of the MK2 and Chk1 mutants indicated in panel A. Wild-type and mutant constructs were transfected into U2OS cells, and live cell images obtained prior to, and 1 hr following, treatment with 10 μM doxorubicin. Of note, inactivation of the NES in MK2 results in a mutant with abolished ability to localize to the cytoplasm following genotoxic stress (compare rows 1 and 3), similar to that seen after inhibition of Crm1-dependent nuclear export of wild-type MK2 with 20 nM leptomycin B (row 2). Fusion of the MK2 NES between GFP and Chk1 produces a mutant that is localized primarily to the cytoplasm (compare rows 4 and 5). This mutant retains the ability to shuttle between nucleus and cytoplasm, as evidenced by nuclear trapping following 12 hr treatment with 20 nM leptomycin B (row 6). A NES-fused Chk1 mutant in which the ATR phosphorylation sites Ser-317 and Ser-345 are mutated to Ala localizes with an identical pattern as the NES-fused wildtype counterpart (rows 7 and 8). Mutational inactivation of the Chk1 NLS produces a mutant that is exclusively localized to the cytoplasm (row 9). This mutant cannot be trapped in the nucleus with leptomycin treatment (row 10).

(C) Functional assessment of the ability of the localization mutants to establish and maintain cell cycle checkpoints. HeLa cells were infected with lentiviruses expressing luciferase control shRNA, MK2-specific shRNA or shRNA targeting

Chk1. Knockdown cells were complemented with the localization mutants as indicated. Cells were treated with doxorubicin in a 30 hr. nocodazole trap experiment and cell cycle profiles were assessed by FACS using phospho-histone H3 staining to monitor the percentage of cells that had escaped doxorubicin-induced cell cycle checkpoints. Loss of nuclear Chk1 could be functionally compensated by expression of the MK2 mutant that was re-targeted to the nucleus (MK2.ΔNES), while loss of cytoplasmic MK2 could be rescued by expression of the Chk1 mutant that was mis-localized to the cytoplasm but retained the ability to shuttle between nucleus and cytoplasm and (GFP.NES.Chk1). A non-activatable Chk1 mutant (GFP.NES.Chk1.AA) or a non-shuttling Chk1 mutant (GFP.Chk1.DNLS) failed to rescue the MK2 RNAi phenotype. Mean values and standard deviations are shown.

Supplemental Experimental Procedures

Chemicals and antibodies

Antibodies against pHH3 were from Upstate. Antibodies detecting Gadd45α, GFP, histone H1, HuR, TIAR and TTP were from Santa Cruz. Anti-Flag (M2) and, β-actin antibodies and IgG were from Sigma. A second anti-GFP antibody and the anti-β-tubulin antibody were from Abcam. The PARN antibodies were purchased from Abnova and Abcam. p38, MK2 and Chk1 antibodies were from Cell Signaling Technology. The anti-HA antibody was purchased from Covance, the anti-6xHis antibody from Quiagen and the GST antibody from GE Healthcare.. Doxorubicin, cisplatin, acetonitrile (HPLC grade), formic acid (HPLC grade), leptomycin B and nocodazole were purchased from Sigma. Propidium iodide and SB203580 were purchased from Calbiochem.

Cell culture and virus production

HEK293T, U2OS and HeLa cells were cultured in DMEM supplemented with 10% FCS, L-Glutamin and penicillin/streptomycin at 37°C in a humidified incubator supplied with 5% CO2. Amphotropic VSV-G pseudotyped lentiviruses encoding the indicated shRNAs were packaged in HEK293T cells using standard procedures (Rubinson et al., 2003), and all subsequent infections were performed in a BL2+ facility. Target cells were infected three times for 12 hr in the presence of 8µg/ml polybrene. Infected cells were selected in 8µg/ml puromycin for 2 days following the last infection.

Plasmids and RNAi

eGFP and eGFP.Gadd45α-3'UTR were a kind gift from M. Gorospe (NIA-IRP, NIH). HA.hnRNP A0, HA.hnRNP A0.S84A, GST.hnRNP A0 and GST.hnRNP A0.S84A were kindly provided by P. Cohen (Dundee). His-tagged PARN in pET33 was kindly provided by A. Virtanen (Uppsala University). Retroviral packaging constructs pMDg and pMDg/p were a kind gift from T. Benzing (Cologne). Lentiviral packaging constructs pRSVrev, pMDg/pRRE and pVSV-G were provided by M. Hemann (MIT). shRNA constructs targeting MK2, Chk1 and luciferase have been described previously (Reinhardt et al., 2007). Gadd45α 29mer shRNA constructs (in pRetroSuper) were obtained from Origene. MK2 and Chk1 eGFP fusion proteins were constructed in the pLNCX-2 (Clontech) retroviral backbone, using standard cloning procedures. GFP-fused MK2 and Chk1 localization constructs were assembled in the pLNCX-2 retroviral backbone. The NES in MK2 was disrupted through mutation of Leu-346 and Met-349 to Ala mutation. The NLS in Chk1 was disrupted through mutation of Arg-260/261/270/271 to Ala mutation. All mutations were generated using the Quickchange mutagenesis kit (Stratagene). N-terminally GFP-fused Cdc25B and C consructs were assembled in the pLNCX-2 backbone using standard cloning procedures. For mammalian expression PARN cDNA was subcloned into pLNCX-2 using standard procedures. TIAR and Hsp25 (AS 71-100, containing the MK2 phosphorylation motive) were subcloned into pGex-4T1 (GE Healthcare) using standard procedures. PARN shRNA was cloned into

pRetroSuper using the oligonucleotides 5'-GAT CCC C**TG GAG ATA ATC AGG AGC AAT T**CA AGA GAT TGC TCC TGA TTA TCT CCA TTT TTG GAA A-3' (forward) and 5'-AGC TTT TCC AAA AAT GGA GAT AAT CAG GAG CAA TCT CTT GAA TTG CTC CTG ATT ATC TCC AGG G-3' (reverse). shRNA-resistant PARN was generated in the pLNCX-2 backbone using the oligonucleotides 5'-GGG GAC TAC AAG GAC GAC GAC GAC AAG ATG GAG AT**T** ATC AGG **TCA** AAT TTT AAG AGT AAT CTT CAC AAA GTG TAC CAG GC-3' (forward) and 5'-GCC TGG TAC ACT TTG TGA AGA TTA CTC TTA AAA TTT GAC CTG ATA ATC TCC ATC TTG TCG TCG TCG TCC TTG TAG TCC CC-3' (reverse). hnRNP A0 shRNA was cloned into pMLP using the oligonucleotides 5'-TGC TGT TGA CAG TGA GCG AAA CGT TTA TGG ATA TCA CAA ATA GTG AAG CCA CAG ATG TAT TTG TGA TAT CCA TAA ACG TTG TGC CTA CTG CCT CGG A-3' (forward) and 5'-TCC GAG GCA GTA GGC ACA ACG TTT ATG GAT ATC ACA AAT ACA TCT GTG GCT TCA CTA TTT GTG ATA TCC ATA AAC GTT TCG CTC ACT GTC AAC AGC A-3' (reverse).

Flow cytometry

Flowcytometry experiments were performed as described earlier (Jiang et al., 2009). In brief, all transfections and treatments were conducted as indicated. Cells were then washed twice in ice-cold PBS, trypsinized and fixed in 70% ethanol overnight at −20°C, permeabilized with PBS containing 0.25% Triton X-100 for 20 min at 4°C, blocked with 2% FCS in PBS, and incubated with 1μg of anti-phospho-histone H3 per 10^6 cells for 180 min at room temperature.

Following extensive washing, cells were incubated with Alexa488-conjugated secondary antibody (Invitrogen) (diluted 1:500 in PBS) for 90 min at room temperature, washed, and resuspended in PBS containing 50 µg/ml propidium iodide and RNAse A prior to analysis on a BD FACScan flow cytometer.

Immunohistochemistry

Formalin-fixed, paraffin embedded sections of human head and neck tumor samples lacking any patient identifying information were obtained from previously evaluated pathological specimens following an IRB-approved protocol. Tissue sections were stained for immunohistochemistry using antibodies against phospho-MAPKAP Kinase2 (pT334-MK2; Cell Signaling Technology), phospho-HSP27 (pS78-HSP27; Epitomics) and γ-H2AX (Millipore). Tissue sections were deparaffinized and rehydrated. Heat-induced epitope retrieval was performed and the tissues were stained with antibodies overnight at 4°C. The Super Sensitive^{TM} IHC Detection System (BioGenex) was used for detection of pMK2, pHSP27 and γ-H2AX. Primary antibodies were omitted for negative control studies. Hematoxylin was used as nuclear counterstain.

Immunofluorescence

Cells were seeded onto 18mm^2 coverslips and either mock treated or treated with doxorubicin for 6 hr. Cells were then fixed in 3% PFA and 2% sucrose for 15 min at RT and permeabilized with 20mM Tris-HCl (pH7.8), 75mM NaCl, 300mM sucrose, 3mM MgCl$_2$, and 0.5% Triton-X-100 for 15min at RT. Cells were stained

with primary antibodies against MK2 or Chk1 at RT for 3 hr. After extensive washing, Alexa-488-conjugated secondary antibodies were used for 3 hrs at RT. Samples were then washed again and counterstained with Hoechst dye. Images were collected on an Axioplan2 microscope (Zeiss) using the Openlab software (Improvision).

Immunoprecipitation

U2OS cells were transfected with HA-tagged Gadd45α or HA-tagged 14-3-3 ζ. 24 hr following transfection, cells were lysed in 50 mM Tris-HCl (pH 7.8), 150 mM NaCl, 1.0% NP-40, 5 mM EDTA, 2 mM DTT, 8 µg/ml pepstatin, 8 µg/ml aprotinin, 8 µg/ml leupeptin, 2 mM Na3VO4, 10 mM NaF, and 1 µM microcystin for 15 min on ice. HA-tagged proteins were immunoprecipitated using protein G beads that were pre-coated with anti-HA antibodies. Immunoprecipitations were carried out for 2 hr at 4°C. Following washing, lysates and bead bound proteins were analyzed by SDS-PAGE, followed by transfer to PVDF membranes, and immunoblotting with the indicated antibodies.

Immunoblotting

Cells were lysed in 1ml of ice-cold lysis buffer (1% Triton X-100, 25mM CHAPS, 20 mM Tris–HCl, pH 7.4, 50 mM NaCl, 50 mM NaF, 15 mM $Na_4P_2O_7$, 2 mM Na_3VO_4 and protease inhibitors) per 10-cm dish for 15 min on ice. Lysates were centrifuged at 4°C for 15 min at 14,000 rpm, and subsequently subjected to ultracentrifugation (100,000 g, 30 min, 4°C). 200 µL of 6x Laemmli buffer was

added to the supernatants and protein concentrations were measured using the BCA Protein Assay Kit (Pierce). 100 µg of each lysate was run on 10% SDS-PAGE and transferred to PVDF (Millipore). The membranes were blocked with 5% BSA in 20 mM Tris- HCl (pH 7.5), 137 mM NaCl, 0.1% Tween-20 and stained with primary antibodies (1:1000 dilution, in TBS-T with 5% BSA) overnight at 4°C. Membranes were then washed in TBS-T and subsequently probed with HRP-conjugated secondary antibody (GE Healthcare) at a 1:5000 dilution and visualized by enhanced chemiluminescence (GE Healthcare). Anti β-actin or anti β-tubulin staining served as a loading control.

In vitro kinase assays

Recombinant 6xHis-tagged wildtype PARN or the SA mutant were expressed in BL21 cells from a pET33 vector, essentially as described previously (Nilsson and Virtanen, 2006). Recombinant GST-tagged hnRNP A0 or the SA mutant as well as recombinant GST, GST-tagged TIAR and Hsp25 (AS 71-100) were expressed from pGEX bacterial expression vectors. *In vitro* kinase assays were performed in identical 30 µl reactions containing 20 mM HEPES (pH 7.5), 10 mM MgCl$_2$, 3 mM β-mercaptoethanol, 100 µg/ml BSA, 50 µM ATP, 10 µCi ^{32}P-©-ATP, and ~10µM His.PARN or GST.hnRNP A0 for the indicated times at 30°C. Recombinant MK2 (Millipore) was used at a concentration of 0.1 µM. *In vitro* kinase assays with GST, GST.TIAR and GST.Hsp25 (AS 71-100) were performed for 20 min in the presence of recombinant MK2 or p38MAPK (Millipore). Reactions were terminated by adding an equal volume of 0.5%

phosphoric acid to the reaction, and the entire reaction was analyzed by 10% SDS PAGE. Autoradiography was performed using Phosphorstorage plates and imaged on the Typhoon Variable Mode Imager station (GE Healthcare).

Mass spectrometric analyses

Immunoprecipitated protein was reduced and alkylated, on beads, in 2 mM DTT and 10 mM iodoacetamide respectively before adding sample buffer and heating at 70°C for 10 minutes. Proteins were resolved on a 4-12% gradient 1.5 mm thick Bis-Tris gel with MES running buffer (Nupage, Invitrogen) and Coomassie stained (Simply Blue, Invitrogen). The gel slices with the approximate molecular weight of PARN were excised from the four lanes, further cut into 1.5 mm cubes and placed into separate microfuge tubes. Protein was digested overnight with trypsin (approximately 0.1 µg enzyme) following standard protocols. Peptides from each gel slice were extracted with 0.1% TFA and cleaned up on C18 StageTips. Peptides were eluted in 50 µL of 80% acetonitrile/0.1% TFA and dried down in an evaporative centrifuge to remove organic solvents. The peptides were then resuspended by vortexing in 7 µL of 0.1% TFA and analyzed by nanoflow-LCMS with an Agilent 1100 with autosampler (HP, Palo Alto, CA) and a LTQ-Orbitrap (Thermo, Bremen Germany). Peptides were resolved on a 10 cm column, made in-house by packing a self-pulled 75 µm I.D. capillary, 15 µm tip (P-2000 laser based puller, Sutter Instruments) column with 3 µm Reprosil-C18-AQ beads (Dr. Maisch GmbH, Ammerbuch-Entringen, Germany) with an analytical flowrate of 200

nL/min and a 58 min linear gradient (~ 0.57 %B/min) from 0.1% formic acid in water to 0.1% formic acid/90% acetonitrile.

We used a data-dependent MS method with Orbitrap full scan (60,000 resolution), LTQ MS^2 and neutral loss-dependent MS^3 scans for the top five most intense precursors from each preceding Orbitrap scan. Data-dependend settings were chosen to trigger an MS^3 scan when a neutral loss of 98.0, 49.0, or 32.7 Da was detected among the three most intense fragment ions. Former target ions selected for MS^2 were dynamically excluded for 30 s. Total cycle time was approximately 3 secs. MS raw files were processed for protein identification and and quantitation with Spectrum Mill (Agilent, VERSION) and IPI human ver.3.32 (http://ebi.ac.uk). Common contaminants like bovine serum albumin, trypsin etc. were also added to the database. Variable modifications used were oxidized methionine, pyroglutamic acid, deamidated asparagine, phosphoserine, phosphothreonine, and phosphotyrosine. Carbamidomethyl-cysteine was a fixed modification. The precursor mass tolerance used in the search was 0.05 Da and fragment mass tolerance was 0.7 Da. Peptides and proteins were autovalidated using default criteria (peptide score > 13, SPI% > 70%, proteins score > 25). This resulted with a FDR < 1% at the peptide level and < 0.01% at the protein level. Extracted ion chromatograms for the PARN peptide, NNSFTAPSTVGKR, in the phosphorylated and unphosphorylated forms were obtained using QualBrowser (Thermo) by defining a mass window +/- 0.01 m/z around the respective peptide m/z.